JAERI - M
83-088

LOSS-OF-FEEDWATER TRANSIENT CALCULATIONS FOR THE ROSA-IV LSTF AND THE REFERENCE PWR WITH RELAP5/MOD1(CYCLE 1)

June 1983

C.P. FINEMAN*, Mitsugu TANAKA
and Kanji TASAKA

日本原子力研究所
Japan Atomic Energy Research Institute

JAERI-M レポートは，日本原子力研究所が不定期に公刊している研究報告書です。
入手の問合わせは，日本原子力研究所技術情報部情報資料課（〒319－11 茨城県那珂郡東海村）あて，お申しこしください。なお，このほかに財団法人原子力弘済会資料センター（〒319－11 茨城県那珂郡東海村日本原子力研究所内）で複写による実費頒布をおこなっております。

JAERI-M reports are issued irregularly.
Inquiries about availabiljty of the reports should be addressed to Information Section, Division of Technical Information, Japan Atomic Energy Research Institute, Tokai-mura, Naka-gun, Ibaraki-ken 319－11, Japan.

編集兼発行　日本原子力研究所
印　　刷　㈱原子力資料サービス

JAERI-M 83-088

Loss-of-Feedwater Transient Calculations for the ROSA-IV LSTF and the Reference PWR with RELAP5/MOD1 (Cycle 1)

C.P. Fineman*, Mitsugu Tanaka and Kanji Tasaka

Department of Nuclear Safety Research,
Tokai Research Establishment, JAERI

(Received May 30 , 1983)

The response of LSTF and the reference PWR to a variety of loss-of-feedwater (LOFW) transients was analyzed with the RELAP5/MOD1, Cycle 1, computer program. The transients analyzed included main feedwater loss only (base case), complete loss-of-feedwater (main and auxiliary), main feedwater loss plus turbine bypass valve failure and main feedwater loss plus primary coolant pump trip at reactor scram. These calculations were the first attempt to analyze the response of LSTF to an operational transient and, therefore, are not a final assessment of the system's capability to represent the PWR response.

Comparison of the results showed that LSTF has the capability to simulate the basic PWR response to the base case LOFW, but with the assumption of an additional failure, there were differences in the response of LSTF and the PWR to the transient. Problem areas identified included the limitation of the core power and primary flow rate to 14% of the respective full-scale value, initial steam generator secondary mass and the method of jet condenser operation. Further study and analysis of the problem areas are recommended in order to find ways to improve the LSTF response relative to the PWR.

Keywords: ROSA-IV, LSTF, PWR, Loss-of-Feedwater, Operational Transient, RELAP5, Computer Analysis, Comparative Evaluation.

---

* USNRC sponsored delegate to the ROSA-IV Program.

ROSA－Ⅳ LSTFとPWRの給水喪失過渡のRELAP5／MOD1(Cycle1)コードによる解析

日本原子力研究所東海研究所安全工学部
C. P. Fineman*・田中　貢・田坂完二

（1983年5月30日受理）

LSTFとPWRの各種の給水喪失過渡（LOFW）の解析をRELAP5／MOD1（Cycle－1）コードで行った。解析したのは主給水のみの喪失（基準ケース），全給水喪失（主給水および補助給水），主給水喪失にタービンバイパス弁の故障が重なった場合，および主給水喪失にひきつづきスクラム時に主冷却ポンプがトリップした場合の4ケースである。これはLSTFの運転上の異常過渡に対する応答を調べた最初の解析であり，LSTFがPWRの挙動をどれだけよく模擬できるかに関する最終的な評価ではない。

計算結果の比較から基準ケースのLOFWに関してはLSTFがPWRの挙動をよく模擬出来ることが明らかとなった。しかし主給水喪失以外の故障をさらに仮定した場合にはLSTFとPWRの挙動に差が生ずる。解析の結果明らかとなった問題点は，炉心出力と流量が定格の14％しかないこと，蒸気発生器2次側の初期水量，およびジェットコンデンサーの運転方法である。これらの点に関してはさらに解析を行い，LSTF実験においてPWR挙動の模擬性を向上することが出来る方法を見い出すことが望まれる。

＊　米国原子力規制委員会の出資でROSA－Ⅳ計画へ派遣された研究員

CONTENTS

目　　次

LIST OF TABLES

LIST OF FIGURES

1. INTRODUCTION

The Japan Atomic Energy Research Institute has initiated the Rig of Safety Assessment, Number 4 (ROSA-IV) program to study the thermal-hydraulics and plant parameters which affect the behavior of a pressurized water reactor (PWR) during a small break loss-of-coolant accident (SBLOCA) or an operational transient. The ROSA-IV program was initiated in response to the accident at Three Mile Island (TMI) which showed the need for more detailed study of these types of accidents and transients. The ROSA-IV program will operate two test facilities. The Two-Phase Flow Test Facility (TPTF)[1] will be used to obtain fundamental two-phase data from separate effects tests in PWR components -- core, horizontal pipe and steam generator. The Large Scale Test Facility (LSTF)[2] will be used to conduct system and integral effects tests. Computer analyses of LSTF used to help in designing the facility and in planning the test matrix are described in this report.

As mentioned above, one of the areas to be investigated with LSTF is PWR behavior during an operational transient. Previous analyses of LSTF and the reference PWR, however, were directed toward the SBLOCA[3,4,5]. Therefore, there was an interest in analyzing the response of LSTF and the reference PWR to an operational transient to evaluate the capability of LSTF to simulate the PWR response. This evaluation was particularly important because LSTF will not be able to simulate full-scaled core power and flow. Because of these limitations, at steadystate LSTF will (1) operate at the maximum core power available, 10 MW (14% of full-scaled core power), (2) maintain the primary loop temperature distribution of the PWR in LSTF by using an initial flow rate which is 14% of full-scaled flow and (3) increase the steam generator secondary pressure to limit steadystate heat transfer to 10 MW. With these differences in initial conditions, method of operation and system capability there was the potential that the LSTF and PWR response to an operational transient would be significantly different. To make an initial evaluation of LSTF, the responses of LSTF and the reference PWR to a variety of loss-of-feedwater (LOFW) transients were analyzed with the RELAP5/MOD1[6], Cycle 1, computer program. The results of these initial analyses are described in this report. These analyses are not a final assessment of the capability of LSTF to represent the PWR response to an operational transient, but should be viewed as a starting point for further study

and analysis.

Section 2 of this report briefly describes the objectives and design philosophy of LSTF. Section 3 describes the analysis models used to perform the calculations, the results of the analyses are contained in Section 4 and Section 5 presents the main conclusions of the study.

2. OBJECTIVES AND DESIGN PHILOSOPHY OF ROSA-IV LSTF

2.1 Objectives

The purpose of tests to be performed at LSTF is to provide test data from a large-scale test facility on the transient performance of PWRs under small break loss-of-coolant accident and transient conditions and to study the effectiveness of emergency safeguard systems and procedures under such conditions. The tests will also provide experimental data on two-phase fluid flow in PWRs. Specifically, LSTF will be used to:

(1) Study the effectiveness of the ECCS under SBLOCA and operational transient conditions. Both standard and potential, alternate ECCS will be evaluated.

(2) Study the effectiveness of secondary side cooling via the steam generators under SBLOCA and operational transient conditions.

(3) Examine the nature of forced and natural circulation cooling in PWRs in various flow regimes and cooling modes and in transition from one flow regime or mode of cooling to another.

(4) Examine the effect of break size and location on system behavior.

(5) Study the effects of non-condensible gases on system behavior during a SBLOCA or operational transient.

(6) Investigate alternate system designs and/or procedures which are being considered to improve system performance during a SBLOCA and/or operational transient.

(7) Provide test data with which to develop/verify the SBLOCA analytical model to be developed in connection with the ROSA-IV Program.

2.2 Design Philosophy

LSTF is an experimental test facility designed to model the full height primary system of a PWR. LSTF will use two equal volume loops to represent the four loops of the referense PWR. Therefore each loop in LSTF represents two loops of the PWR. The reference PWR for LSTF is a 1100 MWe (3423 MWt) PWR with 50,952 fuel pins arranged in 17 × 17 square lattices. The overall scale factor for LSTF is 1/48. LSTF is scaled as follows:

a. Elevations are preserved, i.e., the scaling ratio is 1/1. Preserving correct elevations is important in LSTF, since gravity strongly influences PWR long-term transient behavior, for instance, natural circulation.

b. Volumes are scaled by the facility scale factor of 1/48.

c. Flow Areas in the pressure vessel and steam generators are scaled by the facility scale factors of 1/48 and 1/24, respectively. But the flow area of the primary loop, i.e., the hot-leg and cold-leg, was determined to maintain both volume scaling and the Strouhal number so that flow regime transition could be simulated.

d. Core Power is scaled by the facility scale factor of 1/48 so that the power input per unit volume in the core region is the same as for the reference PWR. Note, for full power operation, the scaled power of the core would be 71 MW. However, heater rod power supply is limited to 10 MW. Hence, proper core power scaling can only be attained for a simulated core power starting at about 14% of full power.

e. Fuel Assembly dimensions, i.e., fuel rod diameter, pitch and length, guide thimble diameter, pitch and length, and the ratio of the number of fuel rods to the number of guide thimbles, are the same as for the 17 × 17 fuel assembly of the reference PWR in order to preserve the heat transfer characteristics of the core. The total number of rods is scaled by the facility scale factor and is 1064 heated and 104 unheated rods.

f. Design Pressures for the LSTF fluid systems will be at least the same as those for their counterparts in the reference PWR.

g. Fluid Flow ΔPs of major components, e.g., pumps, pressure vessel and steam generators will be the same as in the reference PWR.

h. Flow Capacities for LSTF systems are scaled by the power scale factor (1/342) to preserve the enthalpy distribution.

The major characteristics of LSTF are shown in Tables 2.1 and 2.2, a flow diagram is shown in Fig. 2.1 and a plan view of the primary loop is shown in Fig. 2.2.

Table 2.1 Major Characteristics of Large Scale Test Facility (LSTF)

as of January 1983.

COMPONENT		PWR	LSTF	SCALE
PRESSURE VESSEL				
VESSEL INSIDE DIAMETER	(mm)	4394	640	1/6.87
VESSEL THICKNESS	(mm)	220	61	1/3.61
CORE BARREL OUTSIDE DIAMETER	(mm)	3874	534	1/7.25
DOWNCOMER LENGTH	(mm)	6147	6658	1/0.923
DOWNCOMER GAP	(mm)	260	53	1/4.91
DOWNCOMER FLOW AREA	(m^2)	3.38	0.0977	1/34.6
LOWER PLENUM FLUID VOLUME	(m^3)	29.6	0.617	1/48
UPPER PLENUM FLUID VOLUME (NOT INCLUDE UPPER HEAD VOLUME)	(m^3)	28.4	0.490	1/58.0
UPPER HEAD FLUID VOLUME	(m^3)	24.6	0.513	1/48
FUEL (HEATER ROD) ASSEMBLY				
NUMBER OF BUNDLES		193	24	
ROD ARRAY		17 x 17	7 x 7	
ROD HEATED LENGTH	(mm)	3660	3660	1/1
ROD PITCH	(mm)	12.6	12.6	1/1
FUEL ROD OUTSIDE DIAMETER	(mm)	9.5	9.5	1/1
THIMBLE TUBE DIAMETER	(mm)	12.24	12.24	1/1
INSTRUMENT TUBE DIAMETER	(mm)	12.24	12.24	1/1
NUMBER OF HEATER RODS		50952	1064	1/47.9
NUMBER OF NON-HEATING RODS		4825	104	1/46.4
CORE FLOW AREA (WITHOUT SPACER LOCATION)	(m^2)	4.75	0.120	1/39.6
CORE FLOW AREA (WITH SPACER LOCATION)	(m^2)	3.70		
CORE FLUID VOLUME	(m^3)	17.5	0.440	1/39.8
PRIMARY LOOP (SAME 2 LOOPS)				
HOT LEG INSIDE DIAMETER	(mm)	736.6	207	
HOT LEG LENGTH	(mm)	6993	3687	$L/\sqrt{D}$ SIMULATED
CROSSOVER LEG				
INSIDE DIAMETER	(mm)	787.4	168	
LENGTH	(mm)	8346	9547	
COLD LEG INSIDE DIAMETER	(mm)	698.5	207	
COLD LEG LENGTH	(mm)	7207	3438	

Table 2.1 (CONTINUED)

COMPONENT		PWR	LSTF	SCALE
PERSSURIZER				
VESSEL INSIDE DIAMETER	(mm)	2126	600	1/3.54
VESSEL HEIGHT	(mm)	15500	4200	1/3.69
TOTAL VOLUME	(m^3)	51	1.1	1/48
FLUID VOLUME	(m^3)	31	0.65	1/48
ACCUMULATOR (COLD AND HOT)				
VESSEL INSIDE DIAMETR	(mm)	3500	950	1/3.68
VESSEL HEIGHT	(mm)	5280	6600	1/0.80
TOTAL VOLUME	(m^3)	38.2	4.8	1/7.96
LIQUID VOLUME	(m^3)	26.9	3.38	1/7.96
RHR HEAT EXCHANGER				
NUMBER OF TUBES/1PASS		568	24	1/23.7
TOTAL U TUBE LENGTH	(mm)	8600	8600	1/1
TUBE OUTSIDE DIAMETER	(mm)	19.0	19.0	
TUBE INSIDE DIAMETER	(mm)	16.6	15.8	
TUBE WALL THICKNESS	(mm)	1.2	1.6	
TUBE PITCH	(mm)	28.5	28.5	1/1
TUBE ARRAY		Δ	Δ	
HEAT TRANSFER AREA (OUTER SURFACE)	(m^2)	590	25	1/23.6
STEAM GENERATOR (SAME 2 S.G s)				
NUMBER OF TUBES		3382	141	1/24
TUBE LENGTH (AVERAGE)	(m)	20.24	19.71	1/1.03
TUBE OUTSIDE DIAMETER	(mm)	22.2	25.4	
TUBE INSIDE DIAMETER	(mm)	19.6	19.6	1/1
TUBE WALL THICKNESS	(mm)	1.3	2.9	
HEAT TRANSFER AREA (OUTER SURFACE OF TUBE)	(m^2)	4780	221.6	1/21.6
INLET PLENUM VOLUME	(m^3)	4.18	0.174	1/24
OUTLET PLENUM VOLUME	(m^3)	4.18	0.174	1/24
PRIMARY SIDE VOLUME	(m^3)	30.14	1.214	1/24.8
SECONDARY SIDE VOLUME	(m^3)	163.12	6.80	1/24

Table 2.2 Elevation of Each Position

POSITION		PWR	LSTF	SCALE
BOTTOM OF HEATER BUNDLE	(mm)	0	0	
TOP OF HEATER BUNDLE	(mm)	3660	3660	1/1
TOP OF DOWNCOMER	(mm)	4889	5399	1/0.906
BOTTOM OF DOWNCOMER	(mm)	-1259	-1259	1/1
CENTER OF COLD LEG	(mm)	5238	5503	1/0.952
TOP OF COLD LEG INSIDE DIAMETER	(mm)	5588	5606	1/0.997
CENTER OF LOOP SEAL LOWER END	(mm)	2095	1786	1/1.17
BOTTOM OF LOOP SEAL LOWER END	(mm)	1703	1703	1/1
CENTER OF HOT LEG	(mm)	5238	5503	1/0.952
TOP OF HOT LEG INSIDE DIAMETER	(mm)	5606	5606	1/1
BOTTOM OF UPPER CORE PLATE	(mm)	3968	3968	1/1
TOP OF LOWER CORE PLATE	(mm)	109		
BOTTOM OF TUBE SHEET OF STEAM GENERATOR	(mm)	7414	7642	1/0.970
PLENUM LOWER END OF STEAM GENERATOR	(mm)	5819	5819	1/1
TOP OF TUBES OF STEAM GENERATOR	(mm)	18584	18584	1/1

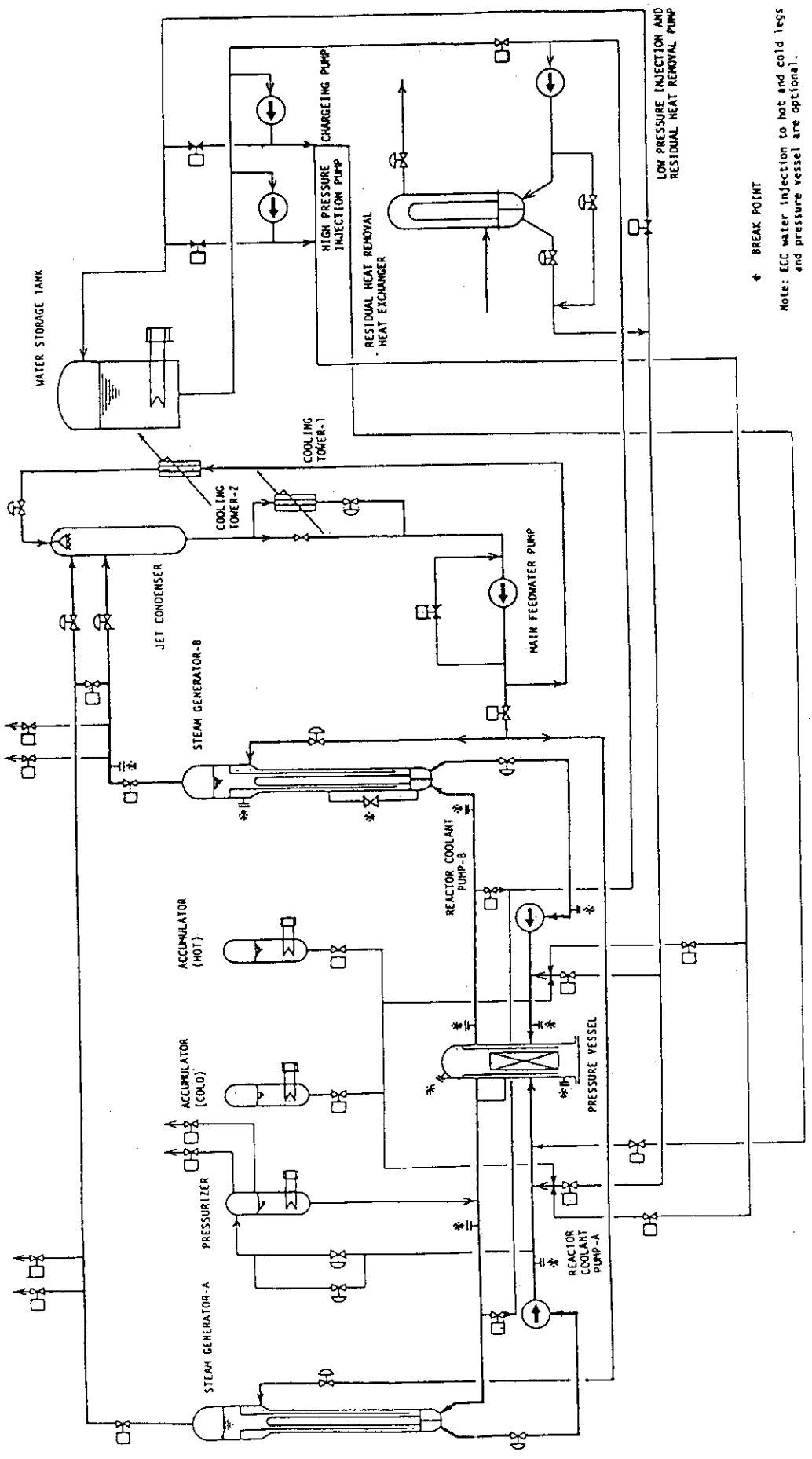

Fig. 2.1 Flow Diagram of LSTF

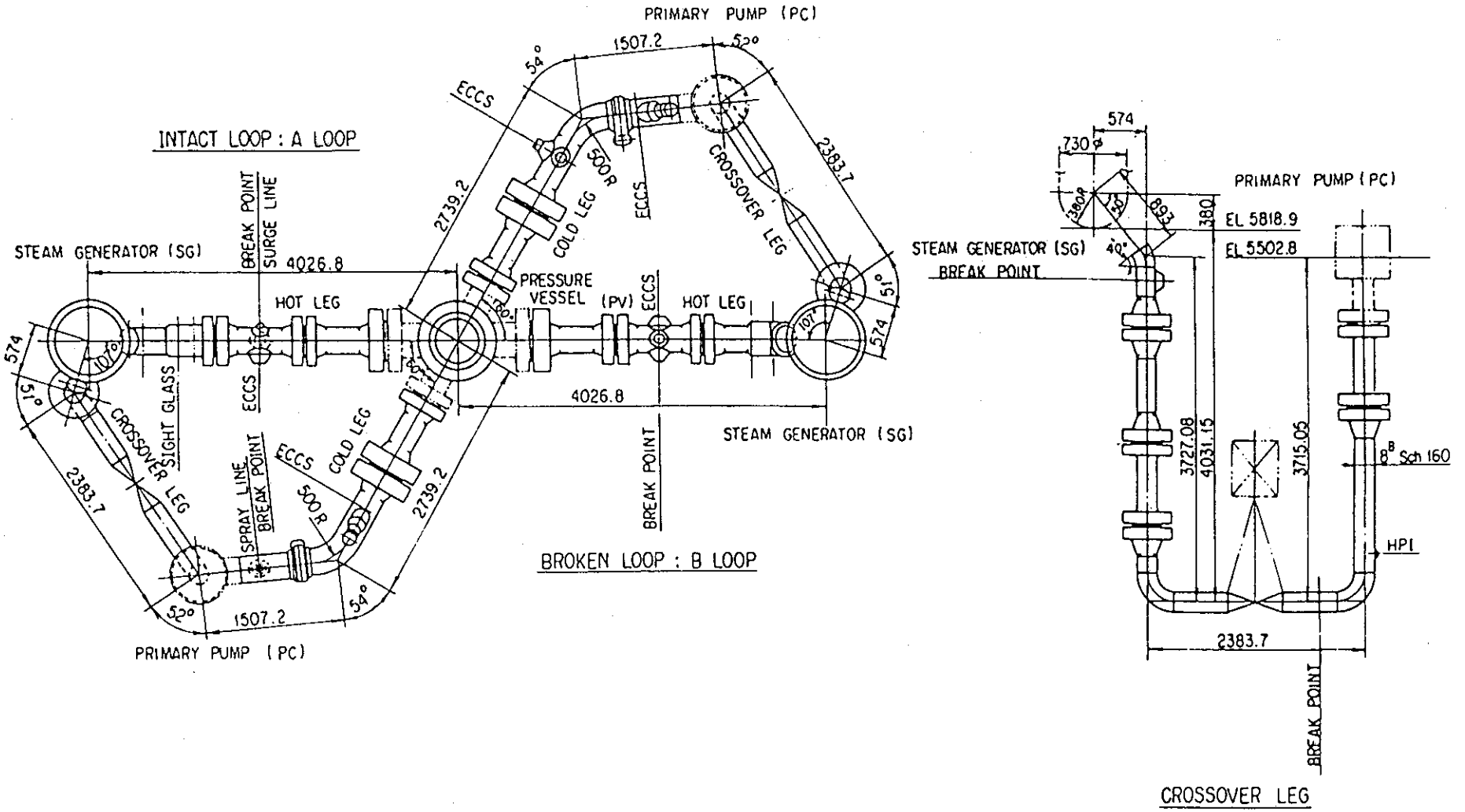

Fig. 2.2 Plan View of Primary Loop of LSTF

3. RELAP5 MODEL DESCRIPTIONS

The RELAP5 models used to make the calculations for LSTF and the reference PWR are described in Sections 3.1 and 3.2, respectively. The trip and control logic for the systems is described in Section 3.3.

3.1 LSTF RELAP5 Model

The RELAP5/MOD1, Cycle 1, model used to represent the LSTF system is shown in Figure 3.1. The model included 190 volumes and 198 junctions. Heat transfer from vessel structures and in the core and steam generators was modeled using 66 heat structures. Steam generator secondary systems, including the jet condenser, were modeled in detail. Since LSTF will have two symmetric loops, both loops in the model are the same except for the location of the pressurizer and the break (if needed).

The RELAP5 control system capability was used to model the control system for the LSTF jet condenser spray and the primary mean temperature control logic for the turbine bypass valve. This is described in detail in Section 3.3.

The initial conditions for the transient calculations were obtained from RELAP5 steady-state calculations. As will be discussed in more detail in Section 4, two sets of initial conditions were used for some of the LSTF calculations. The main difference between the initial conditions was the amount of mass in the steam generator (SG) secondary, but this also caused some differences in the other initial conditions as well. The initial conditions for LSTF1, in Table 3.1, were developed based on maintaining the same initial steam generator downcomer level as in the PWR calculations (approximately 44%). However, because of the smaller core power in LSTF and differences in the steam generator secondary void distribution the secondary mass needed to get a downcomer level of 44% in the LSTF model was greater than that obtained by scaling the secondary mass of the PWR broken loop steam generator by 2/48 (each LSTF steam generator represents two steam generators in the reference plant). This difference was about 520 kg (2150 kg/SG in LSTF1 versus 1630 kg/SG scaled from the PWR) and it became particularly significant in the analysis of the LOFW transient with auxiliary feedwater (aux. FW) failure. The initial conditions for LSTF2, in Table 3.1, were developed

based on maintaining approximately the same secondary mass in the LSTF model as would be obtained by scaling the PWR secondary mass by 2/48, as discussed above. The mass used was approximately 1655 kg/SG in LSTF2 versus the scaled mass of 1630 kg/SG. The resulting steam generator downcomer level was about 12% versus the normal level of 44%. There were small differences in the initial temperatures and pressures between the LSTF calculations and between the LSTF calculations and the PWR model, but these did not affect the transient calculations. There were larger differences in the initial primary flow rate, core power and secondary mass for the three models, and these differences did affect the transient calculations as discussed in Section 4.

3.2 PWR RELAP5 Model

The nodalization diagram for the RELAP5/MOD1, Cycle 1, model used to represent the reference PWR is shown in Figure 3.2. The model included 185 volumes and 192 junctions. Heat transfer in the system was modeled using 72 heat structures. Detailed modeling of the steam generator secondary systems was included up to the turbine throttle and turbine bypass valves. The intact loop represents three loops and the broken loop one loop in the PWR.

To facilitate comparison of the calculated results to those obtained with the LSTF model, as much as possible, the same modeling approach was applied in setting up the PWR model as the LSTF model. Differences in the models occur where a lack of detailed information was faced when modeling the PWR or where the design of the systems is clearly different, as is the case in the secondary systems downstream of the steam generator outlets. In general, however, the description of the LSTF model, above, applies to the PWR model as well.

The initial conditions for the PWR transient calculations were obtained from a RELAP5 steady-state calculation. The initial conditions are listed in Tbale 3.1 for comparison to the LSTF data.

3.3 Trip and Control Logic

The trip logic used in the LSTF and PWR calculations to control the steam generators and the plant protection systems (core trip and emergency core cooling system (ECCS)) was based on the trip logic of

the reference plant. These trips are described in Table 3.2.

The turbine bypass valve (TBV) control logic based on the primary mean temperature was modeled in both the PWR and the LSTF calculations. This logic is designed to use the TBV to maintain a primary mean temperature of 564.9 K after scram by opening or closing the valve depending on whether the mean temperature is above or below this setpoint. The same control system was applied to both systems in the calculations.

The modeling of the TBV is discussed in detail because of the effect it can have on the calculated results. The full open flow area of the TBV in the LSTF models was 1/48 the full open flow area of the TBV in the PWR model. The actual TBV flow area used at a particular time step, however, was directly proportional to the difference between the primary mean temperature and the TBV setpoint (564.9 K plus a delay of 2.78 K before the TBV opens). This was the basis of the control system used to set the TBV flow area in both the LSTF and PWR runs. The primary mean temperature was calculated based on the hot and cold leg temperatures near the vessel nozzles. There was some delay, therefore, equal to the transport time of the fluid from the steam generator outlet to the vessel nozzles before changes in steam generator heat transfer affected the primary mean temperature. Because of the method of jet condenser operation discussed below, the TBV flow rate will also be affected by the pressure difference across the TBV. In general, the pressure difference across the TBV will be less in the LSTF runs than in the PWR runs, where the condenser was modeled as an atmospheric boundary condition.

In the LSTF model, a control system was set up to control the jet condenser spray. In LSTF, the control system will be used to adjust the spray flow rate in order to maintain the jet condenser pressure at its initial value (about 7.07 MPa) during most experiments.

In the calculations where auxiliary feedwater was assumed to be available, the flow rate was controlled to maintain the normal operating level of 44% in the steam generator upper downcomer. This was accomplished by cycling the flow on and off once the downcomer level had recovered to the normal level after the start of the LOFW transient.

Table 3.1 LSTF and PWR Initial Conditions

	LSTF1	LSTF2	PWR
System Pressure (MPa)	15.59	15.59	15.60
Cold Leg Temperature			
Intact Loop (K)	562.31	562.18	562.20
Broken Loop (K)	562.28	562.14	562.22
Hot Leg Temperature			
Intact Loop (K)	598.24	598.15	598.22
Broken Loop (K)	598.24	598.15	598.22
Core Temperature Difference (K)	35.93[a]	35.97[a]	36.02[a]
Core Flow Rate (kg/s)	48.40[b]	48.37[b]	16516.
Core Power (MW)	10.0[b]	10.0[b]	3423.
Steam Generator Secondary			
Intact Loop			
Pressure (MPa)	7.12[c]	7.14[c]	5.71
Mass (kg)	2151.4	1658.9	117043.
Downcomer Level (%)	44.5	11.9	44.8
Broken Loop			
Pressure (MPa)	7.12[c]	7.14[c]	5.71
Mass (kg)	2148.7	1652.0	39068.
Downcomer Level (%)	44.4	11.8	45.0

[a] Based on intact loop data.

[b] Both the initial flow rate and core power are 14% of the full-scaled values based on a system scale factor of 1/48.

[c] The initial SG secondary pressure is higher in LSTF than in the PWR to reduce the steady-state heat transfer to 10 MW.

Table 3.2 Trip Logic

Action	Setpoint
① PWR scram, SG throttle valve closes, turbine bypass valve opens[a]	P < 12.27 MPa[b], P > 16.44 MPa[b] or SG Downcomer level < 25 %[c]
② Trip coolant pump and initiate HPI and safety injection	P < 12.27 MPa[b] or P < 4.235 MPa[d]
③ LSTF core power trip[e]	Scram signal + 7.1 s
④ Aux. FW begins	On loss of main FW[f]
⑤ Main steam isolation valve closes	P < 4.235 MPa[d]
⑥ Steam generator relief valve open	8.03 MPa[d]
close	7.72 MPa[d]

[a] If the primary, mean temperature is above 564.9 K (plus a 2.78 K delay), the turbine bypass valve opens, otherwise it is closed.

[b] Pressurizer pressure

[c] Collapsed liquid level in upper SG downcomer less than 25% of full-scale.

[d] Steam generator secondary steam dome pressure

[e] The PWR core power decreases to 14% power level in 7.1 s after scram. The LSTF steady state power level corresponds to 14% of the PWR one. In the calculations using initial conditions LSTF2 in Table 3.1 (SG secondary mass scaled from the PWR calculation), the core power in the LSTF was tripped at approximately 20 s based on the PWR calculations. The reason for this is discussed in Section 4.

[f] As a simplifying assumption, and until more information is obtained from the reference PWR, no delay in aux. FW initiation was assumed.

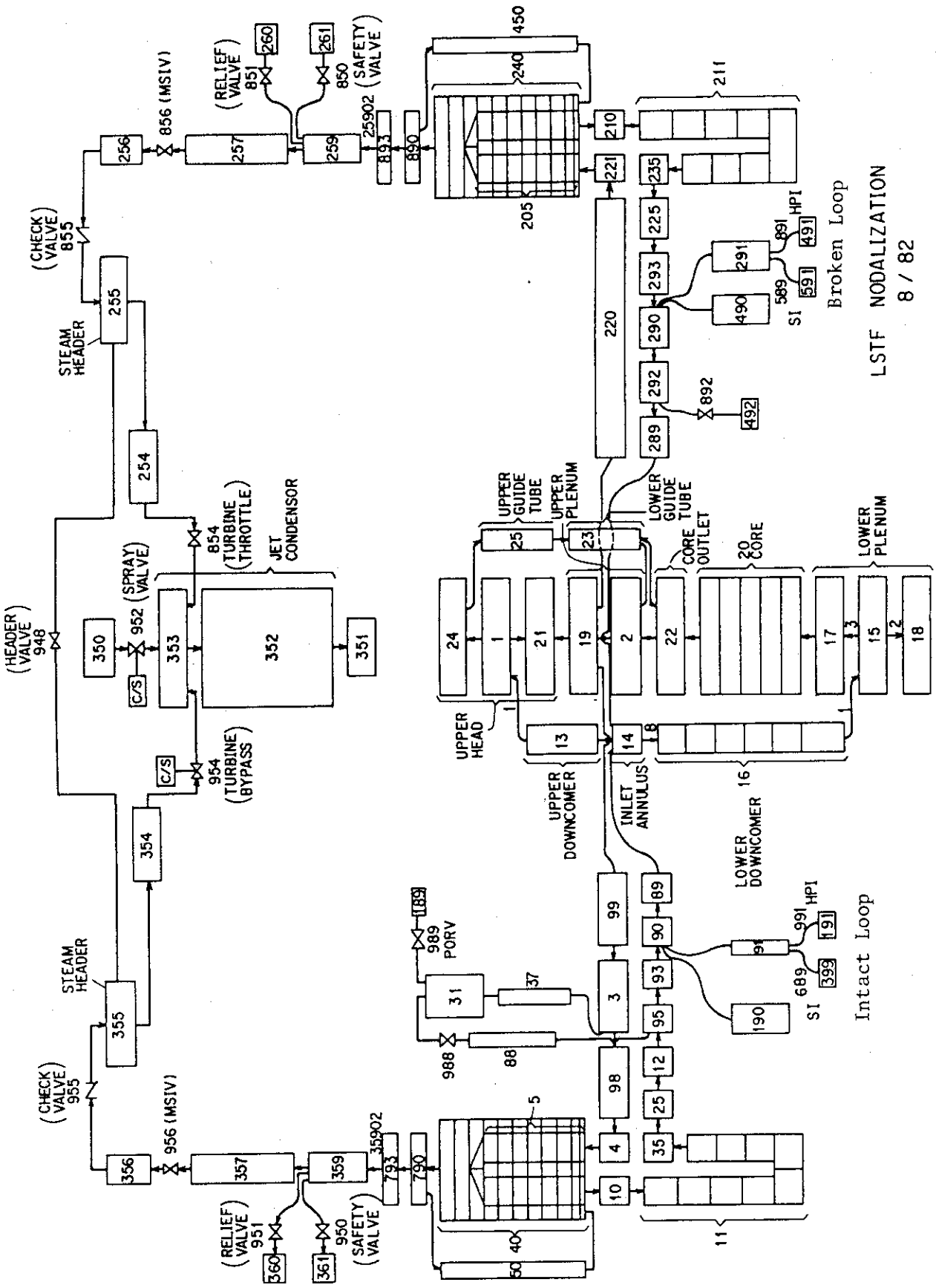

Fig. 3.1 Nodalization of LSTF

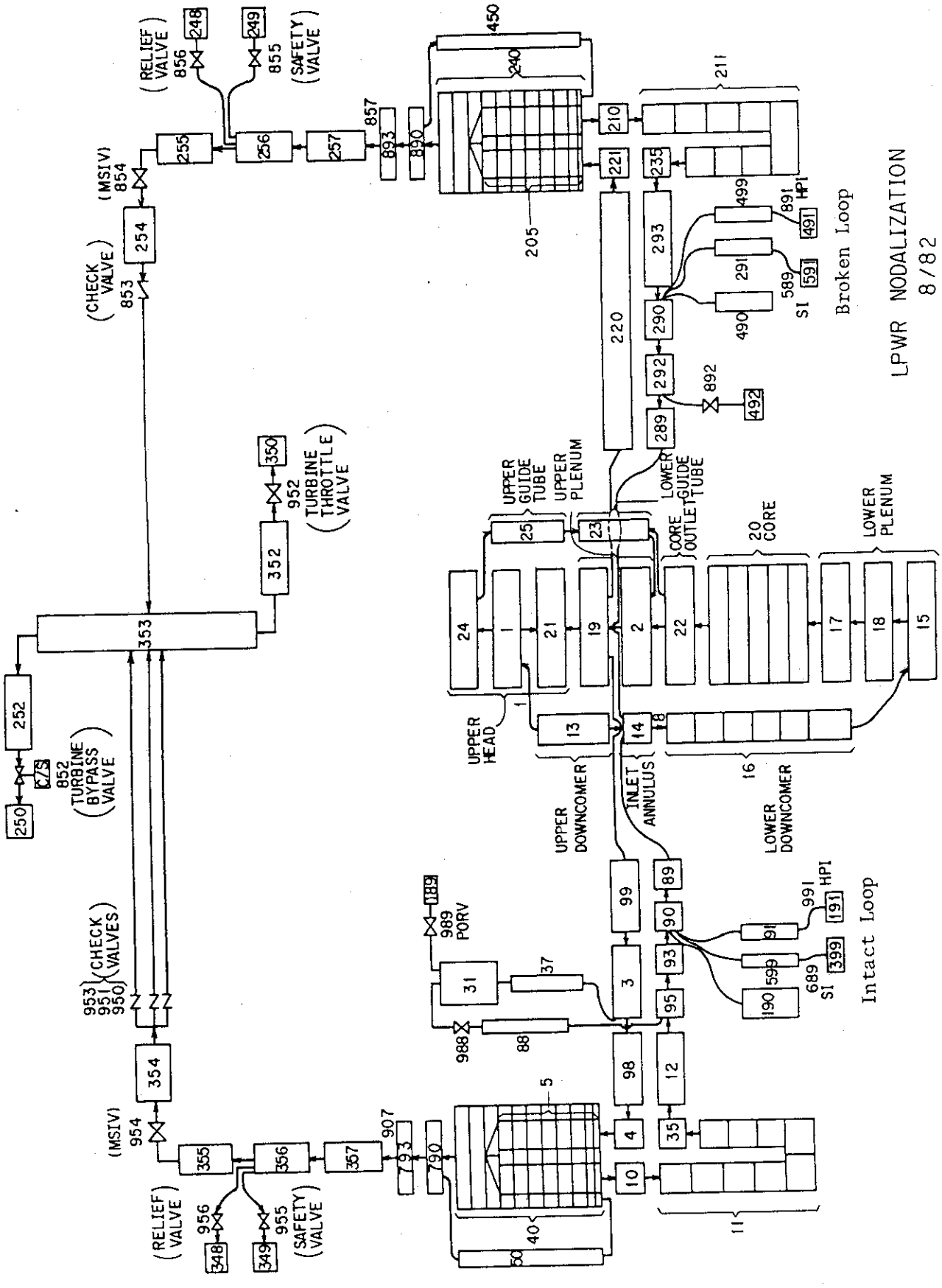

Fig. 3.2 Nodalization of PWR

4. Analyses of Calculated Results

The matrix for the LOFW analyses completed as part of this study is shown in Table 4.1. In Table 4.1, LSTF1 refers to the LSTF model with the correct steam generator downcomer level, but the larger than scaled secondary mass, and LSTF2 refers to the LSTF model with the correctly scaled mass, but low downcomer level. This matrix was developed based on the initial calculations for LOFW-A (the base case analysis) and LOFW-B with the LSTF1 and PWR models. The analysis of LOFW-B with these models indicated the time to steam generator dryout was significantly different because of the larger than scaled secondary mass in the LSTF1 model. This showed the need for an analysis with an LSTF model using the correctly scaled secondary mass (LSTF2) for the LOFW-B transient and also LOFW-A, to determine the effect of secondary mass on the base case. Because of the importance of the turbine bypass valve in controlling the LOFW-A transient, an analysis of a LOFW with turbine bypass valve failure (LOFW-C) was made. Also in analyzing LOFW-A, differences in the results for LSTF and the PWR were found which were due to differences in the primary flow rate. Since the pump capacity in LSTF will not be sufficient to match the PWR flow rate, calculations were completed where the pumps were tripped on reactor scram (LOFW-D). Reactor scram was chosen for the pump trip so that scram would occur because of a low steam generator downcomer level as in the other calculations. An earlier pump trip would probably have caused a scram on high primary pressure or low primary flow.

The analyses of LOFW-A to LOFW-D are discussed in Sections 4.1 to 4.4, respectively.

4.1 Analysis of LOFW-A

LOFW-A was the base case LOFW analysis. In this analysis, the main feedwater to all steam generators was assumed to be lost at the beginning of the calculation and all other systems, including the aux. FW system, were assumed to operate as designed. This LOFW transient was analyzed with LSTF1 (large SG secondary mass), LSTF2 (scaled SG secondary mass) and the PWR model.

The response of the steam generator secondary pressure in the three calculations to the LOFW-A transient is shown in Figure 4.1.

In the PWR calculation, scram occurred at 14.2 s on a low SG level and the secondary pressure rapidly increased as the turbine throttle valve closed. As the core power decreased, the aux. FW was able to cool the secondary and the pressure began to decrease. At approximately 1050 s, the level in the steam generator downcomer recovered to the normal operating level of 44% and the aux. FW began to cycle on and off to maintain that level. With the aux. FW cycling, the pressure in the secondary began to increase. As the secondary pressure increased, the primary mean temperature also increased (see Figure 4.2) until, at 1330 s, the turbine bypass valve (see Figure 4.3) setpoint was exceeded and the valve opened. The turbine bypass valve remained open for the remainder of the calculation, controlling the secondary pressure and the primary mean temperature through a secondary feed and bleed - feed through the aux. FW and bleed through the turbine bypass valve.

The response of LSTF1 and LSTF2 to LOFW-A was basically the same except for the timing of events because of differences in the time of PWR scram and the initial secondary mass. Scram occurred at 161 s in LSTF1 because of a low steam generator level and at 14.2 s in LSTF2 because of trip input. The reason for this difference is discussed below. At the time of core scram, the secondary pressure in both LSTF calculations did not increase rapidly as in the PWR calculation. This was because the turbine bypass valve remainded open longer than in the PWR calculation (see Figure 4.3) because of the slower cooldown rate of the primary fluid as seen in Figure 4.2. This was due to the smaller than scaled flow rate in LSTF. With the smaller than scaled primary flow rate, the hot leg fluid temperature did not decrease as rapidly as in the PWR once the core scrammed. Since the fluid cooled at a slower rate, the primary mean temperature decreased at a slower rate and the TBV remained open longer. As the primary mean temperature dropped due to the core power decay, the TBV closed and the secondary pressure in both LSTF calculations decreased as a result of the aux. FW cooling the secondary. At 710 s in LSTF1 and 850 s in LSTF2, the downcomer level recovered to normal (44%) and the aux. FW began to cycle. As in the PWR calculation, the secondary pressures began to increase until, at 850 s in LSTF1 and 1150 s in LSTF2, the primary mean temperature had increased to the turbine bypass valve setpoint and the valve opened (see Figures 4.2 and 4.3). The TBV then controlled the secondary pressure to maintain the primary mean temperature through a secondary feed and bleed.

The final secondary pressure in the two LSTF calculations was lower than in the PWR case. This was also due to the smaller than scaled flow in LSTF. At a given core power the smaller flow in the LSTF calculations resulted in a larger core temperature difference. Therefore, since the final primary mean temperature was the same in all the calculations (see Figure 4.2), the hot and cold leg fluid temperatures in LSTF1 and LSTF2 were higher and lower than the corresponding temperatures in the PWR. In order to get a lower cold leg temperature in the LSTF runs, the secondary pressure had to be lower than in the PWR analysis.

Table 4.2 compares the calculated sequence of events for the three analyses of LOFW-A. This table summarizes the differences in the timing of events as calculated by the three models. The estimated secondary mass balance shown in Table 4.3 is helpful in understanding these differences between the calculations.

In the case of the PWR and LSTF1, PWR scram was calculated to occur because of a low steam generator downcomer level. This occurred at 14.2 s in the PWR calculation and at 161.0 s in the calculation for LSTF1 (see Table 4.2). Table 4.3 indicates the mass lost from the steam generators prior to PWR scram was about the same in the LSTF1 and PWR analyses, although it took longer for this to occur in LSTF1. There were two reasons for this. First, with the core power in LSTF1 limited to 10 MW (14% of full-scaled power), it took longer to boil off the mass. The second reason was the aux. FW flow rate used in the LSTF1 analysis. This flow rate was 2/48 of the aux. FW flow in one PWR steam generator and it was not adjusted for the smaller core power in LSTF. The aux. FW flow in LSTF1 was therefore, about 42% of the steady-state main FW flow rate. This compares to an aux. FW flow rate in the PWR analysis which was 6% of the steady-state main FW flow. Thus, before scram more mass was added to the steam generator per unit of core power in the LSTF1 calculation than in the PWR calculation and this increased the time required to reach the SG level scram setpoint.

In LSTF2, the PWR scram was set to occur at 14.2 s by trip input. The normal steam generator level in the PWR is 44% and scram occurs on a low level of 25%, a difference of 19%. In LSTF2, with the SG mass scaled from the PWR calculation, the initial level in the steam generator downcomer was about 12% because of differences in the

secondary void distribution due to the smaller core power. Since this level was lower than the trip setpoint for scram, the simplest approach was to input in LSTF2 the time of PWR scram based on the analysis with the PWR model. If an initial steam generator mass similar to that in LSTF2 is to actually be used in the LSTF facility, then some care must be taken in selecting the scram trip logic.

The differences between the calculations in the time the SG level recovered to normal and the aux. FW began to cycle, shown in Table 4.2, were due to differences in the secondary mass at scram (see Table 4.3). Since all the analyses had about the same secondary mass at the time the SG level recovered, the time to level recovery increased with decreasing secondary mass at scram because it took longer to refill the steam generator. Even though the LSTF1 and PWR analyses lost about the same mass prior to scram, LSTF1 had a larger mass inventory at scram because of a larger, initial secondary mass. LSTF1 also had a larger mass inventory at scram than LSTF2 because, although LSTF2 lost less mass prior to scram, the difference in initial inventories more than compensated for it. Finally, LSTF2 had a larger secondary mass at scram than the PWR because less mass was lost prior to scram due to the smaller than full-scaled core power.

The calculated primary pressure response to LOFW-A for the PWR, LSTF1 and LSTF2 is shown in Figure 4.4. The same basic response is seen in all three analyses although the timing is different for the same reasons as discussed above. At scram, the primary pressure decreased in all three calculations. In the PWR analysis, however, the initial decrease was more rapid and larger than in either of the LSTF runs. This difference in the initial pressure response was due to flow rate differences between the PWR and LSTF. With the smaller than full scale flow in LSTF1 and LSTF2, the hot leg fluid temperature did not decrease as rapidly at scram in these calculations as in the PWR analysis. Since the fluid cooled at a slower rate, the fluid specific volume decreased more slowly than in the PWR run and, therefore, the system pressure decreased at a slower rate. In response to the secondary pressure, the primary pressure increased in the PWR run before turning over. All the primary pressures decreased until the normal steam generator level was recovered, when they began to increase in response to the increase in the secondary pressures. The primary pressures plateaued in all the analyses when the TBVs opened to maintain the primary mean

temperature.

The calculations were ended when the system response in each of them had stabilized. Although there were differences in the final primary and secondary pressures between the PWR and LSTF calculations, the calculations showed both LSTF and the PWR reached a hot standby condition which was maintained by a secondary feed and bleed.

4.2 Analysis of LOFW-B

In LOFW-B, a loss of both the main and auxiliary feedwater systems was assumed. This transient was analyzed with the same three models as LOFW-A: LSTF1 (large SG secondary mass), LSTF2 (scaled SG secondary mass) and the PWR model.

Table 4.4 compares the calculated sequence of events for the three analyses. In the LSTF1 and PWR calculations, scram occurred because of a low steam generator level signal. The time of the scram signal was different (79 s versus 11 s) because with the smaller than scaled core power in LSTF it took longer to boil off the mass in the LSTF1 calculation than in the PWR run. The time of PWR scram in LSTF2 was set by trip input to be the same as in the PWR calculation for the reasons discussed in the analysis of LOFW-A.

The time of steam generator dryout differred in the three analyses and reflected the difference in steam generator mass inventory at scram as shown in the estimated mass balance in Table 4.5. The mass inventories at scram differred from each other for the same reasons as in the LOFW-A analysis. The more mass left in the steam generators at scram, the longer it took to dryout. This was due not only to the greater mass inventory, but also to the core power decay. That is, any additional mass to be boiled off, relative to the mass in the PWR calculation, would have been boiled off at a lower core power which would have added to the time required for dryout to occur. A second factor was the greater energy addition to the primary fluid by the PWR pumps when compared to the LSTF pumps. The greater energy addition in the PWR calculation would also lead to an earlier SG dryout.

The steam generator secondary pressures for LSTF1, LSTF2 and the PWR are shown in Figures 4.5 and 4.6. In the PWR calculation, the pressure increased at scram as the throttle valve was closed. The pressure plateaued at about 7.8 MPa when the turbine bypass valve opened because

the primary mean temperature exceeded the setpoint (see Figures 4.7 and 4.8). When the steam generators dried out at about 1500 s, the PWR pressure decreased rapidly to the setpoint for main steam isolation valve (MSIV) closure, 4.235 MPa, because there was no more liquid to heat to steam.

The secondary pressure response in LSTF1 and LSTF2 was essentially the same except for the timing of events (due to differences in the time for scram and initial mass inventory). The oscillations in the secondary pressures for these calculations were due to the turbine bypass valve opening and closing (see Figure 4.7). The turbine bypass valve opened and closed in the LSTF analyses, but not in the PWR analysis, because of the smaller than scaled primary flow in LSTF. The smaller flow in the LSTF runs slowed the response of the primary mean temperature (which was the variable input to the TBV control system) to changes in the turbine bypass valve flow area, so that the primary mean temperature tended to over- and undershoot the setpoint for the TBV (see Figure 4.8). This over- and undershoot in the primary mean temperature caused the secondary pressure to oscillate as it was fed back into the TBV control system. In the PWR calculation, however, the correct primary flow rate enabled the turbine bypass valve to maintain the primary mean temperature constant. With a constant primary mean temperature, no pressure oscillations were calculated in the PWR run.

It was also noted the LSTF analyses of LOFW-A did not calculate significant oscillations in the secondary pressure and the primary mean temperature, even though the smaller than scaled primary flow was also modeled in those runs. Since the same control system for the turbine bypass valve was used in both transients, this difference was attributed to the method of jet condenser operation modeled in the two transients. In general, the LSTF jet condenser pressure is to be held constant at the initial pressure throughout an experiment. This initial pressure has been about 7.07 MPa. This method of jet condenser operation was modeled in the LSTF analyses of LOFW-A. In the analyses of LOFW-B with LSTF1 and LSTF2, however, the jet condenser pressure was reduced to about 3.0 MPa at reactor scram in order to calculate the rapid secondary pressure decrease when the steam generator dried out. This could not have been done if the jet condenser pressure had been held constant at 7.07 MPa throughout the calculation. The differential pressure across the turbine bypass valve was, therefore,

about 4.0 MPa larger in the LOFW-B calculations than in those for LOFW-A. The larger pressure difference gave larger TBV flow rates for a given TBV flow area and, thus, greater energy removal in LOFW-B when compared to LOFW-A. In the LOFW-B calculations, this caused the primary mean temperature to undershoot the TBV setpoint and, as this was fed back to the TBV control system, oscillations in the primary mean temperature and the secondary pressure were calculated. The smaller pressure difference in the LOFW-A calculations thus prevented significant oscillations from occurring in the LOFW-A runs even though the smaller than scaled flow was inherent in both transients.

The secondary pressure in the LSTF calculations decreased rapidly at the time of steam generator dryout until the MSIV closed. The time of dryout was different (2783 s in LSTF1 and 2066 s in LSTF2) relative to each other and the PWR calculation for the reasons discussed above. The secondary pressures in LSTF1 at about 3700 s, and in LSTF2 at 3200 s (intact loop) and 4200 s (broken loop) increased rapidly (see Figures 4.5 and 4.6). This was due to the rapid vaporization of a small amount of liquid trapped in the SG after it was isolated when the MSIV closed. In both LSTF1 and LSTF2 this liquid was in the separator and upper downcomer volumes.

In the three calculations, the primary pressure response was controlled by the turbine bypass valve operation after scram occurred. This is shown in Figure 4.9 which compares the calculated primary pressures for the LOFW-B runs. The difference in the pressure decrease at scram between the PWR run and the LSTF runs was a result of the smaller than scaled flow rate in LSTF as discussed in the analysis of LOFW-A. The pressure plateaued in the PWR run once the turbine bypass valve opened at 80 s while the oscillations in the pressure in the LSTF analyses were due to the TBV opening and closing as discussed above. In all the calculations, once the steam generators dried out, the primary pressure increased to the PORV setpoint (16.20 MPa) because the secondary heat sink was lost. The PORV cycled for the remainder of the transient in all the calculations.

High pressure injection (HPI) was initiated and the primary coolant pumps tripped[a] in all the analyses when the secondary pressure decreased to the setpoint for MSIV closure. The primary energy removal mechanism, once SG dry out had occurred, thus became primary feed and bleed —— feed through the HPI system and bleed through the PORV as it cycled. As shown in the comparison of the primary mean temperature (Figure 4.8), however, the energy balance was not sufficient to prevent the primary fluid from heating up. With the earlier steam generator dry out in the PWR analysis, the mean temperature increased to a higher temperature than in the LSTF runs. In all the calculations, however, the fluid remained subcooled and no voiding was calculated to occur. The maximum hot leg temperature reached in the PWR analysis was approximately 611 K, which was about 11 K subcooled at the PORV setpoint. The maximum hot leg temperatures in LSTF1 and LSTF2 were 598 K and 605 K, respectively. The heatup rate of the primary fluid in the LSTF analyses was slightly greater than that calculated in the PWR run. One possible reason for this was the use of heat structures to model the heat transfer capability of the pressure vessel wall in the PWR analysis but not in the LSTF runs. These heat structures were calculated to be a heat sink after SG dryout in the PWR run. Thus, these heat structures provided an additional heat sink in the PWR run not found in the LSTF runs, and therefore the primary fluid heated up at a slower rate.

The calculations were ended at 6000 s because the end of the input core power table was reached. The primary fluid in all the analyses was subcooled at this time and no voiding in the primary system had occurred.

---

[a] For these calculations, an input table of pump speed versus time was used to model the pump coastdown. In the PWR analysis the pump speed was assumed to go to zero 200 s after the pump was tripped. In the LSTF analyses, the pump speed was held constant until the pump speed intersected the pump coastdown curve of the PWR (66 s after trip). The LSTF pumps then followed the same coastdown curve as the PWR.

4.3 Analysis of LOFW-C

The transient analyzed as LOFW-C was the same as LOFW-A except the turbine bypass valve was assumed to fail. This transient was analyzed with only two models, LSTF1 and the PWR. Table 4.6 shows the calculated sequence of events.

At scram, the throttle valves were closed in both calculations and the pressures increased rapidly. The secondary pressures for the two analyses are shown in Figure 4.10. The time of scram was different for the reasons discussed in the LOFW-A analysis. In the LSTF calculations for LOFW-A and LOFW-B the secondary pressure did not increase at scram because the turbine bypass valve opened and removed energy from the secondary as discussed before. In LOFW-C the TBV was not available and since this prevented energy removal from the secondary, the pressure increased. With the initial, higher secondary pressure in LSTF1, the pressure increased to the steam generator relief valve setpoint at about 300 s, before the aux. FW began to cool the secondary. The calculated PWR secondary response to this transient was the same as that for LOFW-A, at scram the pressure increased as the throttle valve was closed before turning over because of aux. FW cooling the secondary.

At about 590 s in LSTF1 and approximately 1070 s in the PWR calculation, the normal steam generator level was recovered and the aux. FW began to cycle on and off to maintain that level. The difference in the timing of this event was because of mass inventory differences at scram as in LOFW-A. With the aux. FW cycling, the secondary pressure increased in both runs until the steam generator relief valve setpoint (8.03 MPa) was reached. The relief valve then cycled for the remainder of the calculation as it alone was sufficient to remove the core decay heat.

Since the secondary pressure in both calculations was maintained at the same value by the relief valve, the final average primary temperature for LSTF1 and the PWR were different (see Figure 4.11) because of the smaller than scaled flow rate in LSTF1. With the same secondary pressure, the temperature at the bottom of the core in the two runs was the same (see Figure 4.12), but with the smaller flow rate in LSTF1, the core temperature difference was larger and therefore LSTF1 had a higher mean temperature.

The primary pressure in both calculations decreased at scram (see Figure 4.13) with the pressure decrease in the PWR run being larger and more rapid than in LSTF1 for the same reason as before. In addition, the pressure in LSTF1 did not decrease as far as in the other transients discussed. With the secondary pressure increasing at scram in LOFW-C (whereas it was constant in LOFW-A and LOFW-B), the pressure at which the primary and secondary came into equilibrium was higher in this transient than the others. After scram, the primary pressure in both calculations, in general, increased and decreased with the secondary pressure. One exception to this was the pressure increase at 250 s in LSTF1, which was caused by the primary to secondary heat transfer dropping below the energy input by the core (see Figure 4.14). The pressure turned over when the relief valves in the secondary opened at 300 s.

Once the secondary pressure increased to the SG relief valve setpoint, the primary pressure in LSTF1 remained relatively constant for the remainder of the transient. The PWR calculation, however, indicated the pressure would oscillate as the relief valve cycled and, overall, the pressure had a downward trend. The oscillations in the pressure were caused by oscillations in the primary mean temperature (see Figure 4.11) as the relief valve cycled and their effect on the pressurizer level (Figure 4.15). The oscillations were larger in the PWR analysis than in LSTF1 because of larger heat removal from the primary system as the relief valve cycled (see Figure 4.16). Possible reasons for this difference are the differences in primary flow rate and the thicker steam generator tubes planned for use in LSTF (see Table 2.1). The downward trend in the PWR pressure, as it oscillated, is thought to be due to condensation in the pressurizer as the level oscillated (as discussed above). In general, a rising pressurizer level, as seen in Figure 4.15, results in a primary pressure increase, however, in this case the pressure decreased. This, taken together with the fact that the primary mean temperature was constant, indicated that the level increase and pressure decrease were due to condensation in the pressurizer. The condensation was caused by subcooled liquid which entered the pressurizer as it emptied and refilled during the transient and replaced the saturated liquid initially in the pressurizer.

It is interesting to note that the pressurizer liquid in the LSTF1 calculation had significantly less subcooling at the end of the run

than the pressurizer liquid in the PWR calculation because of the smaller changes in pressurizer level during the transient. The smaller amount of subcooling in the LSTF1 pressurizer fluid indicates there was less potential for condensation in the pressurizer to cause a pressure decrease in the LSTF run than in the PWR run. Even if oscillations similar to those in the PWR analysis after 1300 s had been calculated by LSTF1, the pressure decrease in LSTF1 would probably have been less than in the PWR because of the smaller subcooling.

The calculations were ended when they indicated the system response had stabilized. The primary systems in both calculations were essentially in a hot-standby condition and were cooled by a secondary feed and bleed - feed through the aux. FW and bleed through the relief valve.

4.4 Analysis of LOFW-D

The LOFW-D transient was the same as LOFW-A except the pumps were tripped at PWR scram to study the influence of primary flow rate on the system response. This transient was analyzed with the LSTF1 and PWR models. The calculated sequence of events is shown in Table 4.7.

The secondary pressure response as calculated by LSTF1 and the PWR model were significantly different. Figure 4.17 shows the secondary pressures calculated by the LSTF1 and the PWR models. The secondary pressure response calculated by LSTF1 was basically the same as in LOFW-A, although the final secondary pressure was lower in LOFW-D than in LOFW-A. The final secondary pressure was lower because, with the pumps tripped, the smaller primary flow rate resulted in a larger core temperature difference. In order to maintain the primary mean temperature at the TBV setpoint, a lower cold leg temperaure was required and therefore, the secondary pressure was lower.

In the PWR analysis, the secondary pressure increased at scram as the steam generator throttle valve was closed but, turned over more rapidly than in LOFW-A because, with the smaller primary flow rate in LOFW-D, heat transfer to the secondary was less. The smaller primary flow rate in LOFW-D also resulted in a higher primary mean temperature so that at 160 s and 275 s the turbine bypass valve opened (see Figure 4.18) and the secondary pressure decreased. After 400 s, the pressure decreased as the secondary was cooled by the aux. FW. At 1140 s, the steam generator level had recovered to normal and the aux. FW began

to cycle to maintain it at that level. The pressure then increased until, at 1650 s, the primary mean temperature exceeded the turbine bypass valve setpoint (see Figure 4.19) and the TBV opened decreasing the secondary pressure. The affect of the TBV opening was more pronounced in the PWR calculation of LOFW-D, compared to LOFW-A, because the smaller primary flow rate with the pumps tripped increased the response time for the control system of the TBV. The affect of the smaller primary flow rate was less in the LSTF1 run because of the smaller pressure difference across the TBV with the jet condenser pressure held constant at its initial value.

Because of the differences in the secondary response in the LSTF1 and the PWR calculations, the primary pressure response was also different. The primary pressure essentially followed the secondary pressure during the transient as seen in Figure 4.20. The pressure increase in LSTF between 300 and 400 s was due to the heat transfer to the secondary dropping below the energy input by the core. At 1820 s in the PWR calculation, the primary pressure decreased to the ECCS trip point and HPI injection began. The injection rate was sufficient to cool the fluid (see the primary mean temperature in Figure 4.19) but the system pressure increased because the pressurizer level rose (Figure 4.21) (due to HPI injection) and compressed the vapor space.

The jet condenser pressure in the LSTF1 run was maintained by the pressure control system at its initial value throughout the calculation as will be the usual mode of operation in LSTF. This affected the results of LSTF1, however, between 300 and 800 s. Figure 4.18 shows the TBV flow rate for the two calculations and indicates the TBV flow was negative between 300 and 380 s and was zero between 420 s and about 780 s. This was due to the calculated SG pressure dropping below the jet condenser pressure so there was negative flow between 300 and 380 s and the check valves in the steam line closed between 420 and 780 s. As a result, although the turbine bypass valve was open, it was not available for energy removal from the system. This affected the secondary pressure response in LSTF1 and, therefore, the primary pressure and primary mean temperature response as well. Had the TBV been able to perform in LSTF1 as designed, the calculated response would probably have been closer to that obtained with the PWR model.

The calculations were ended after the ECCS trip occurred in the PWR run and it was clear the LSTF1 calculation would not calculate this trip.

Table 4.1 Loss-of-Feedwater Calculation Matrix

Model \ LOFW	A	B	C	D
LSTF1	X	X	X	X
LSTF2	X	X		
PWR	X	X	X	X

LOFW-A: LOFW with aux. FW available (Base Case)
LOFW-B: LOFW with aux. FW failure
LOFW-C: LOFW with aux. FW but turbine bypass valve failure.
LOFW-D: LOFW with aux. FW but pump trip on reactor scram

All other systems worked as designed in the above calculations.

Table 4.2 Calculated Sequence of Events - LOFW-A

	Event	Time (s)		
		PWR	LSTF1	LSTF2
1.	Aux. FW Began	0.0	0.0	0.0
2.	Scram (PWR)	14.2	161.0	14.2[a]
3.	LSTF Power Trip	-	168.2	21.3
4.	SG Level Recovered to Normal/Aux. FW Began to Cycle	1050.0	710.0	850.0
5.	Turbine Bypass Valve Opened Second Time	1333.0	850.0	1150.0

[a] PWR scram was set to occur at the same time as in the PWR calculation by trip input.

Table 4.3 Estimated Secondary Mass - LOFW-A

Model	Initial SG Mass	SG Mass Lost Prior to Scram[a]	SG Mass at Scram[b]	SG Mass when Aux. FW Began to Cycle[c]
LSTF1	2150	254.7	1895	2536
LSTF2	1655	22.5	1632	2608
1/24 PWR	1630	261.4	1369	2586

[a] Estimated from (Initial flow-Aux. FW flow) × Time to Scram

[b] Estimated from Initial SG Mass - SG Mass Lost Prior to Scram

[c] Estimated from SG Mass at Scram + (Aux. FW flow × ④ - ② of Table 4.2))

Table 4.4 Calculated Sequence of Events - LOFW-B

Event	Time (s) PWR	LSTF1	LSTF2
1. Scram (PWR)	10.95	78.94	11.0[a]
2. LSTF Power Trip	—	86.06	18.1
3. SG Dryout	1566.7	2783.0	2066.0
4. HPI Came On	1566.7	2783.0	2066.0
5. PORV Began to Cycle	1725.0	2875.0	2200.0

[a] PWR scram set by trip input.

Table 4.5 Estimated Secondary Mass Balance - LOFW-B

Model	Initial SG Mass	SG Mass Lost Prior to Scram[a]	SG Mass at Scram[b]
LSTF1	2150	217	1933
LSTF2	1655	30	1625
1/24 PWR	1630	315	1415

[a] Estimated from Initial flow × time to scram

[b] Estimated from Initial Mass - Mass Lost Prior to Scram

Table 4.6 Calculated Sequence of Events - LOFW-C

Event	Time (s) PWR	LSTF1
1. Aux. FW on	0.0	0.0
2. Scram (PWR)	15.55	158.4
3. LSTF Power Trip	-	165.5
4. SG Level Recovered to Normal/Aux. FW Began to Cycle	1070.0	590.0
5. SG Relief Valve Began to Cycle	1314.0	720.0[a]

[a] The relief valve cycled once at about 300 s before the secondary pressure turned over due to aux. FW flow.

Table 4.7 Calculated Sequence of Events - LOFW-D

Event	Time (s) PWR	LSTF1
1. Aux. FW on	0.0	0.0
2. Scram (PWR)	15.5	158.4
3. Primary Pump Trip	15.5	158.4
4. LSTF Power Trip	—	165.6
5. SG Level Recovered to Normal/Aux. FW Began to Cycle	1140.0	720.0
6. Turbine Bypass Valve Opened Second Time	1648.0	[a]

[a] In the LSTF1 calculation, the turbine bypass valve opened at the time of PWR scram (158.4 s) and remained open for the remainder of the calculation.

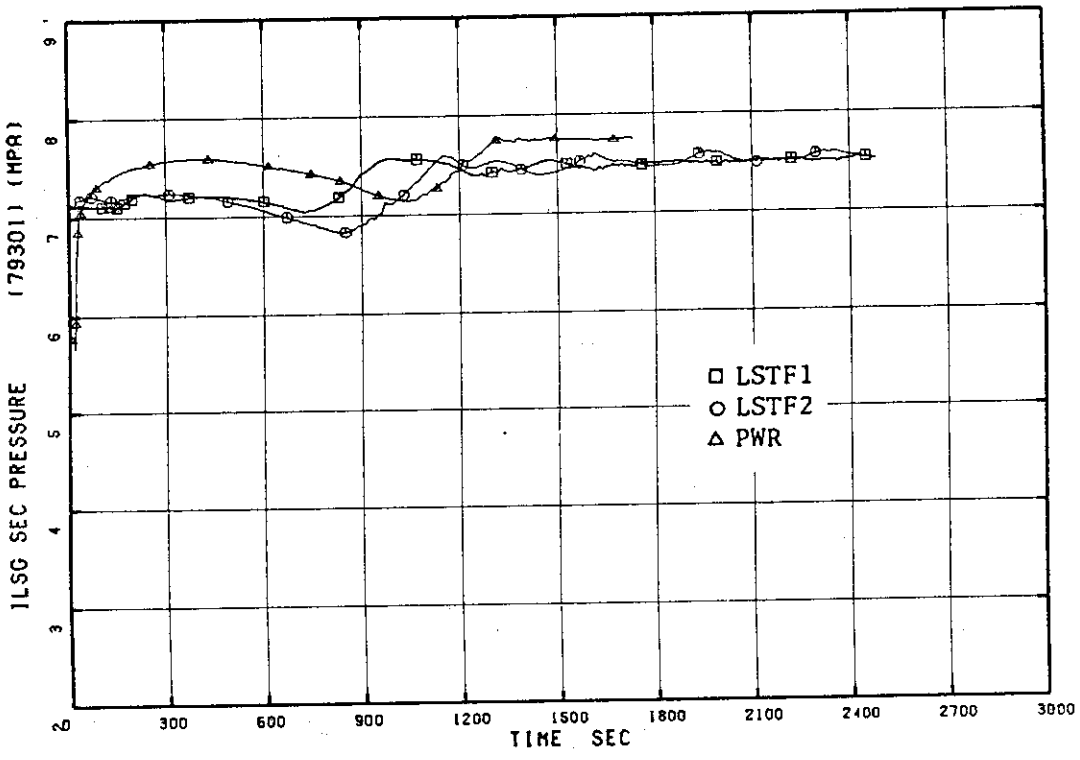

Fig. 4.1 Intact Loop Steam Generator Secondary Pressure - LOFW-A

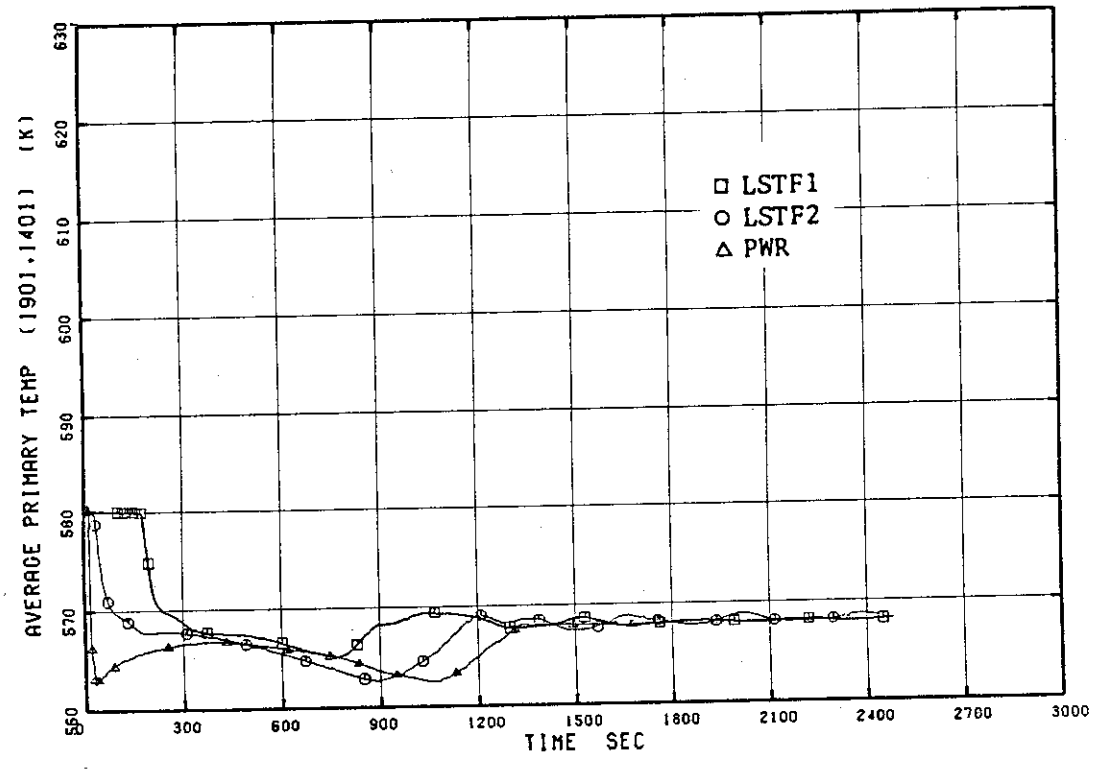

Fig. 4.2 Primary Mean Temperature - LOFW-A

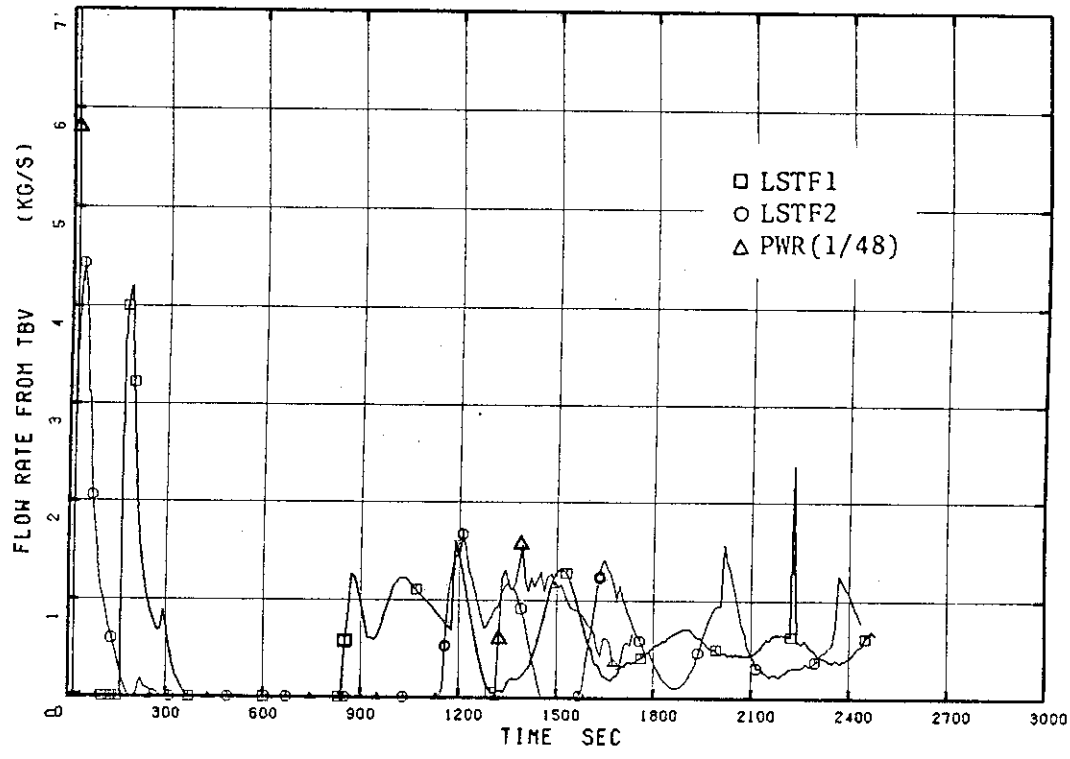

Fig. 4.3 Turbine Bypass Valve Flow Rate - LOFW-A

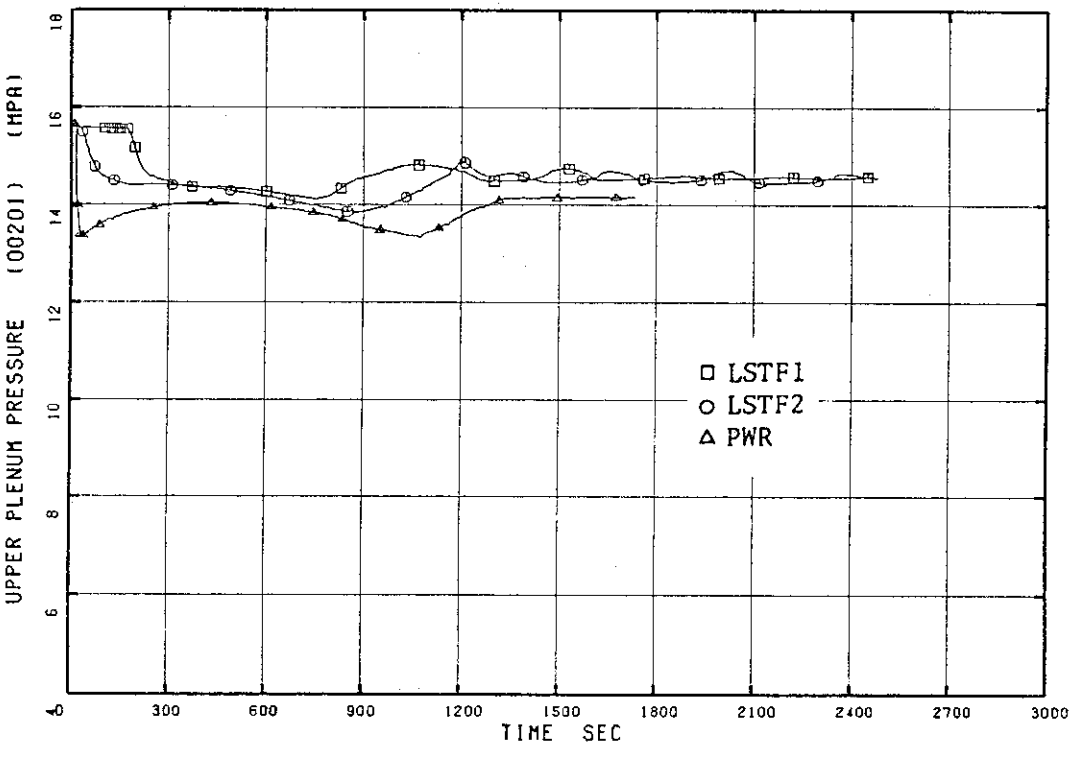

Fig. 4.4 Upper Plenum Pressure - LOFW-A

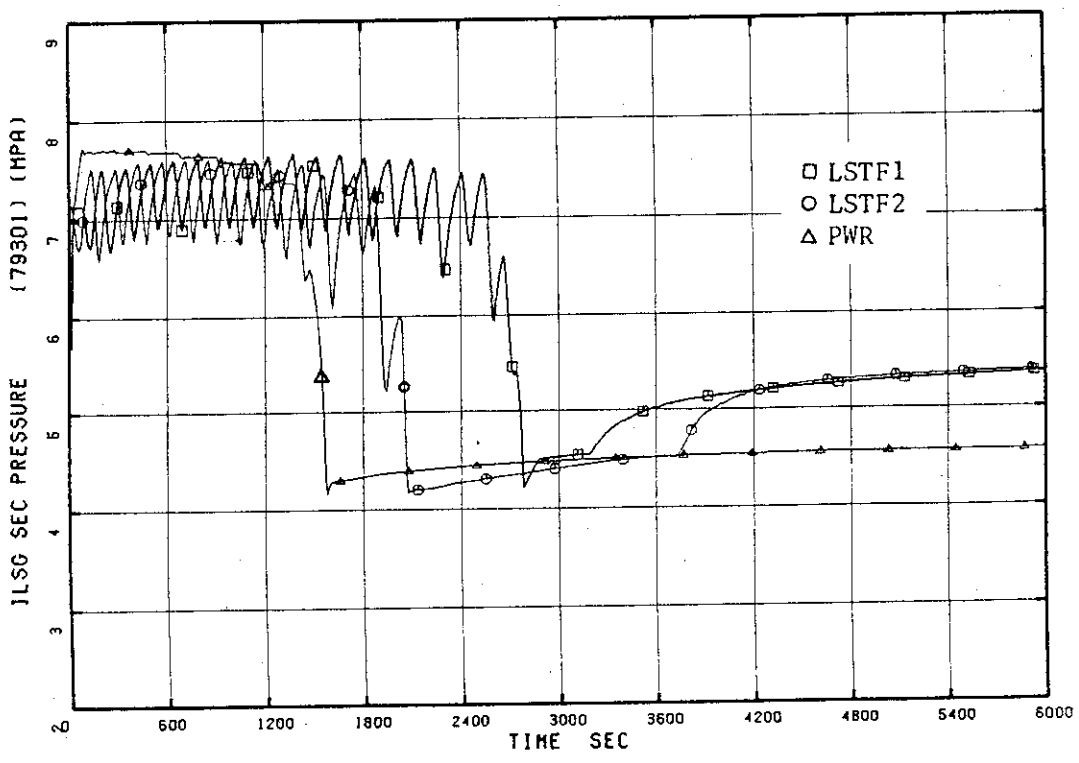

Fig. 4.5 Intact Loop Steam Generator Secondary Pressure - LOFW-B

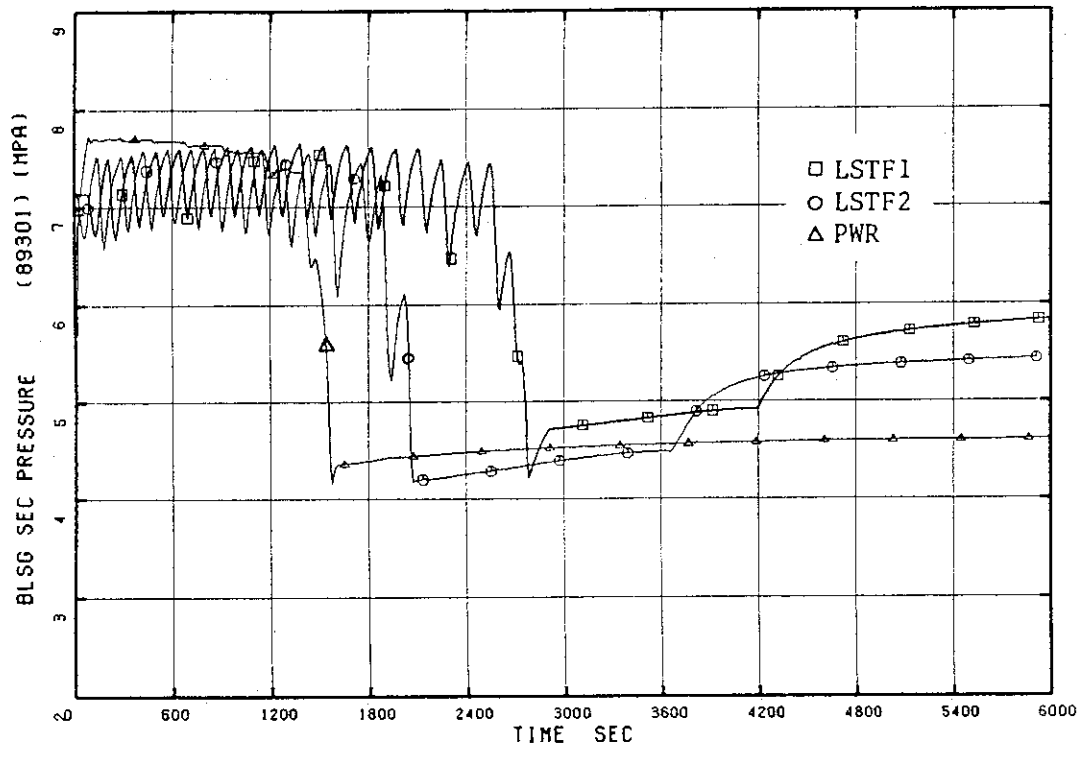

Fig. 4.6 Broken Loop Steam Generator Secondary Pressure - LOFW-B

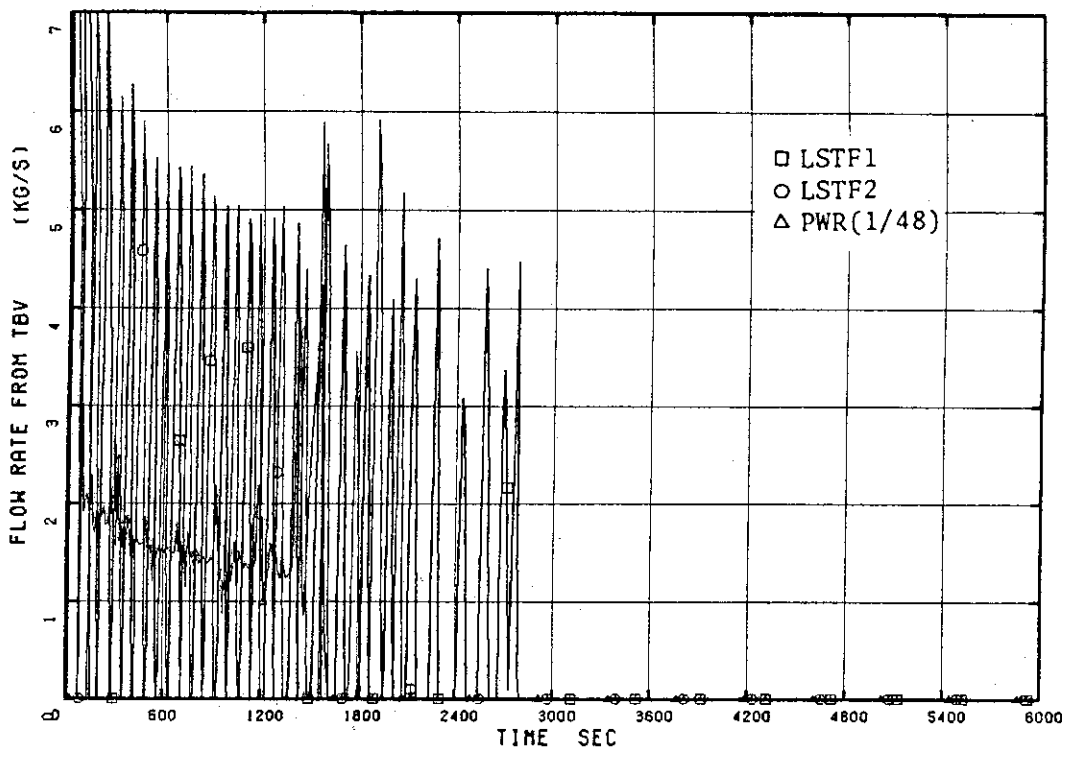

Fig. 4.7 Turbine Bypass Valve Flow Rate - LOFW-B

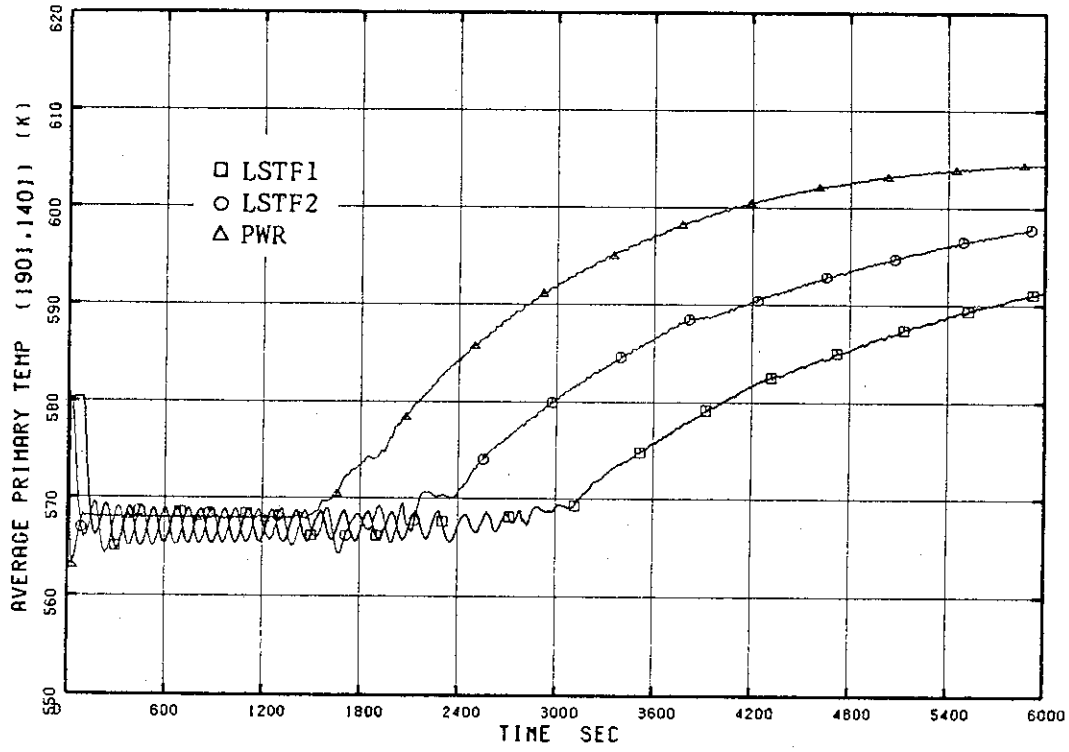

Fig. 4.8 Primary Mean Temperature - LOFW-B

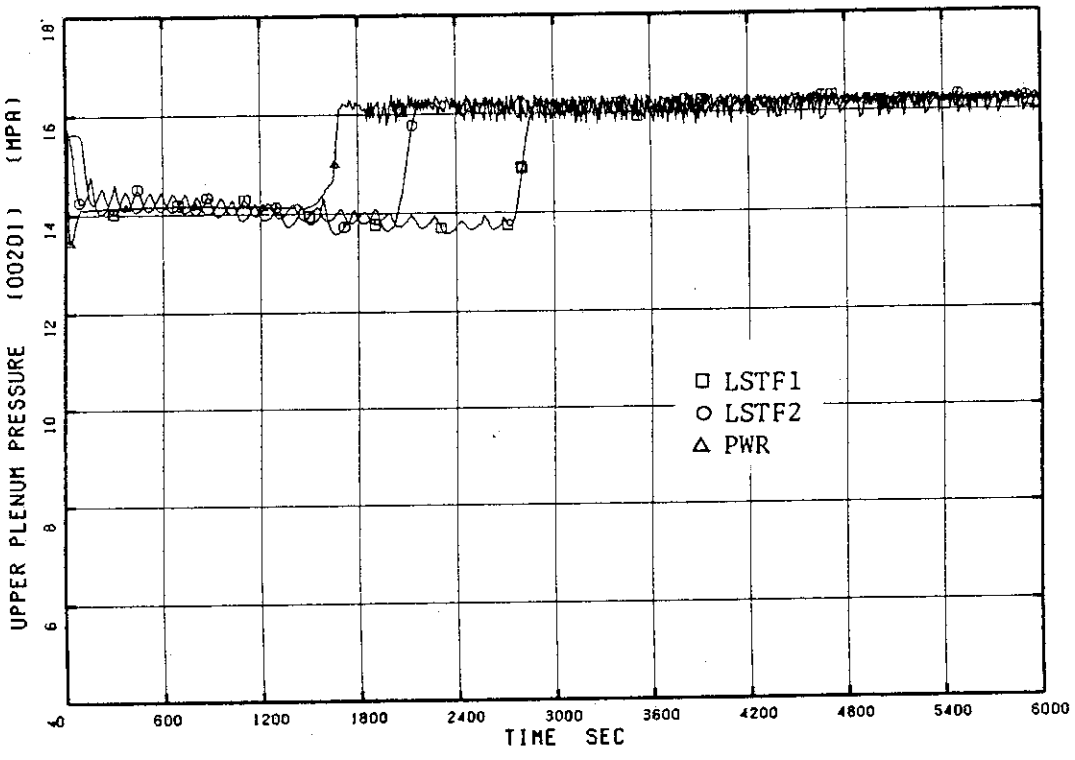

Fig. 4.9 Upper Plenum Pressure - LOFW-B

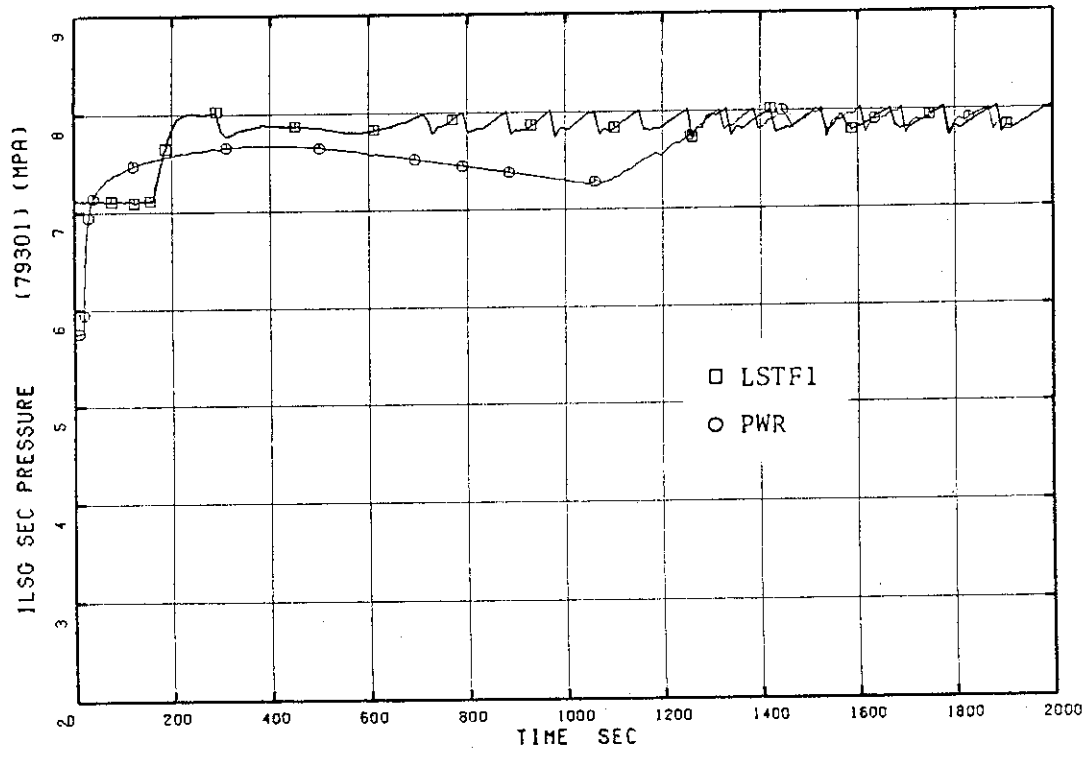

Fig. 4.10 Intact Loop Steam Generator Secondary Pressure - LOFW-C

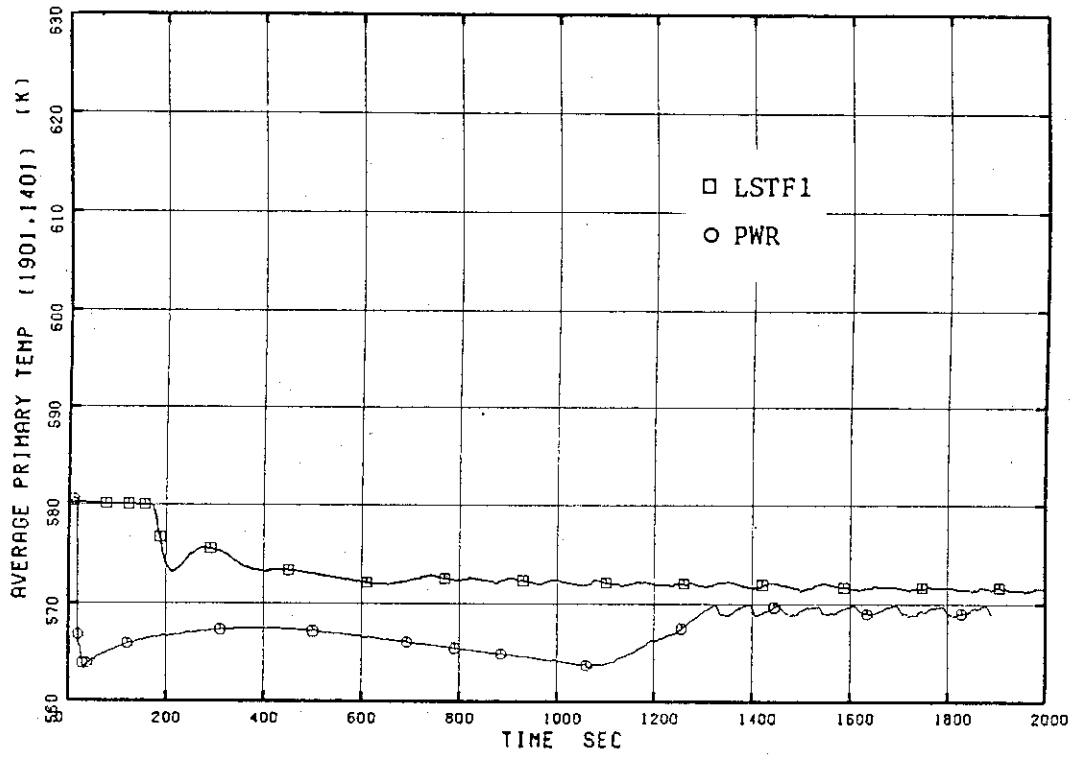

Fig. 4.11 Primary Mean Temperature - LOFW-C

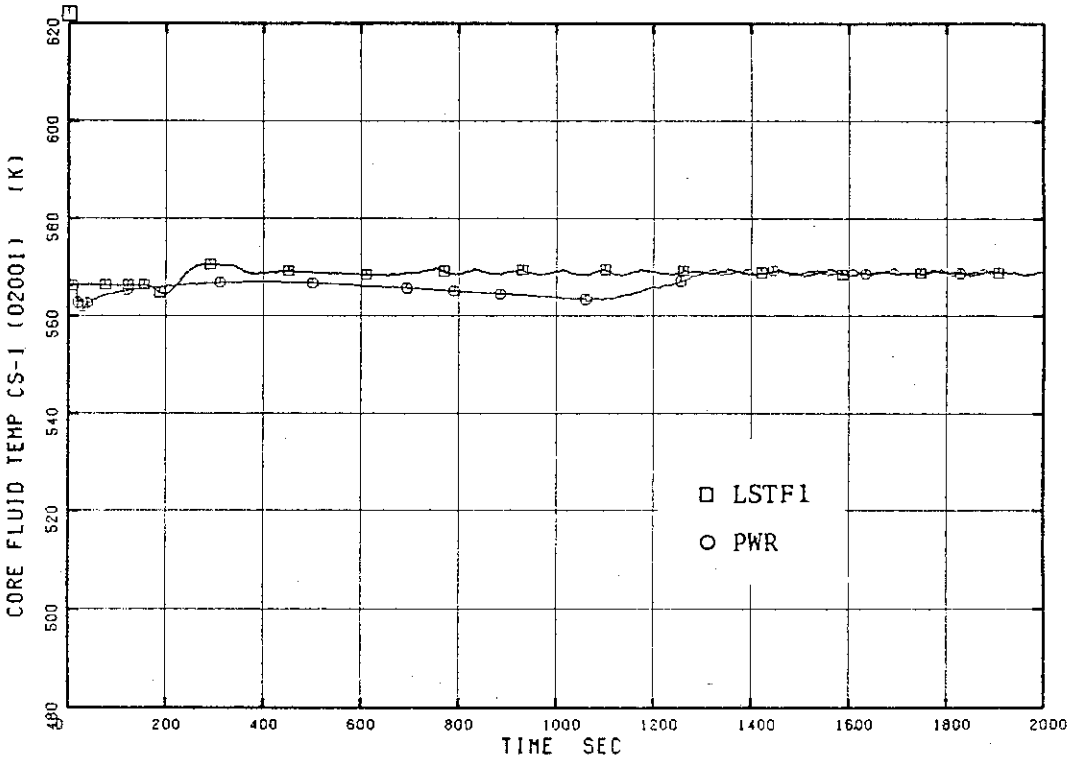

Fig. 4.12 Fluid Temperature at the bottom of the Core - LOFW-C

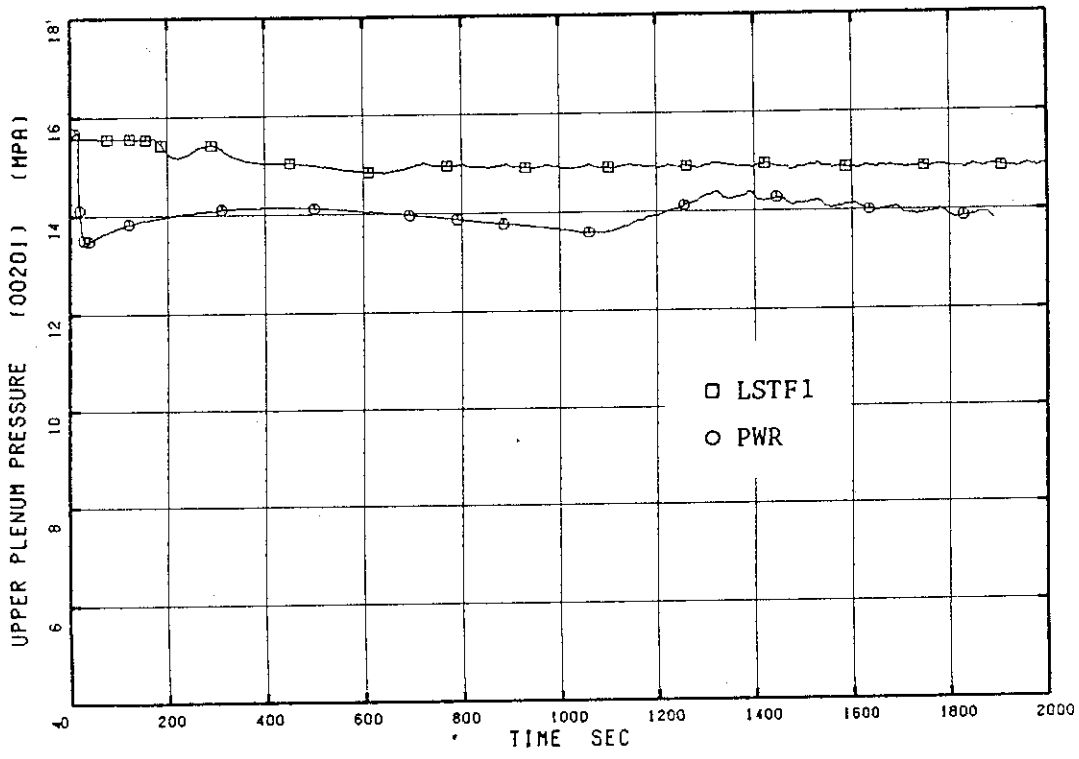

Fig. 4.13 Upper Plenum Pressure - LOFW-C

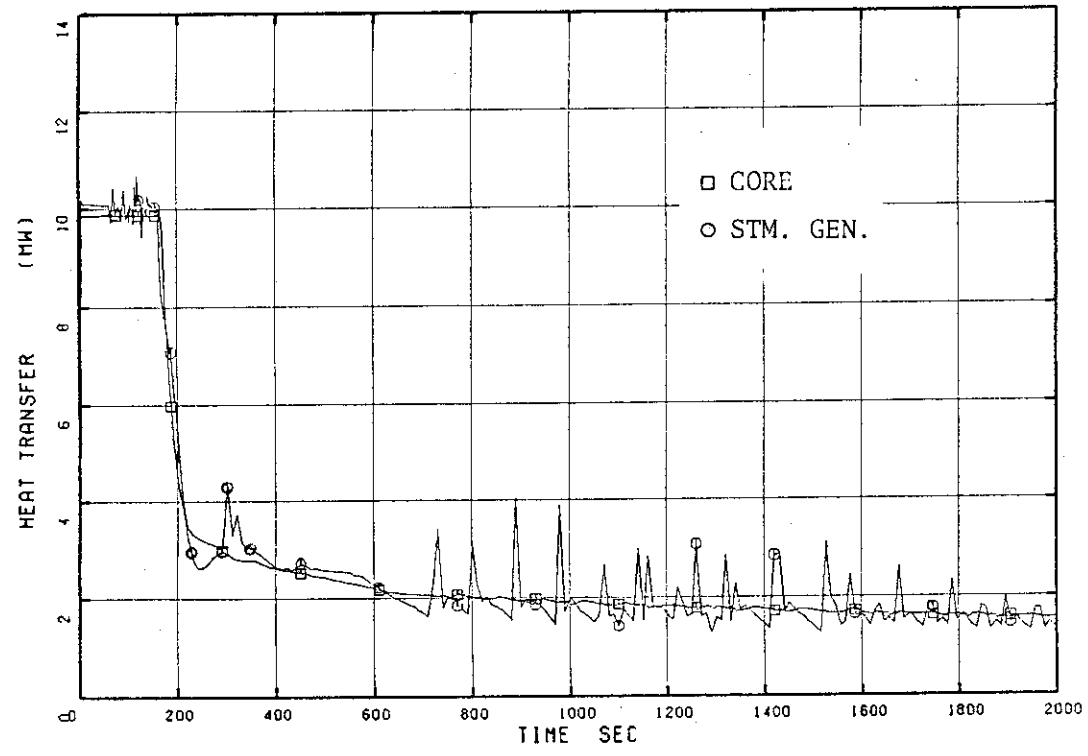

Fig. 4.14 Comparison of LSTF1 Core and Steam Generator Heat Transfer - LOFW-C

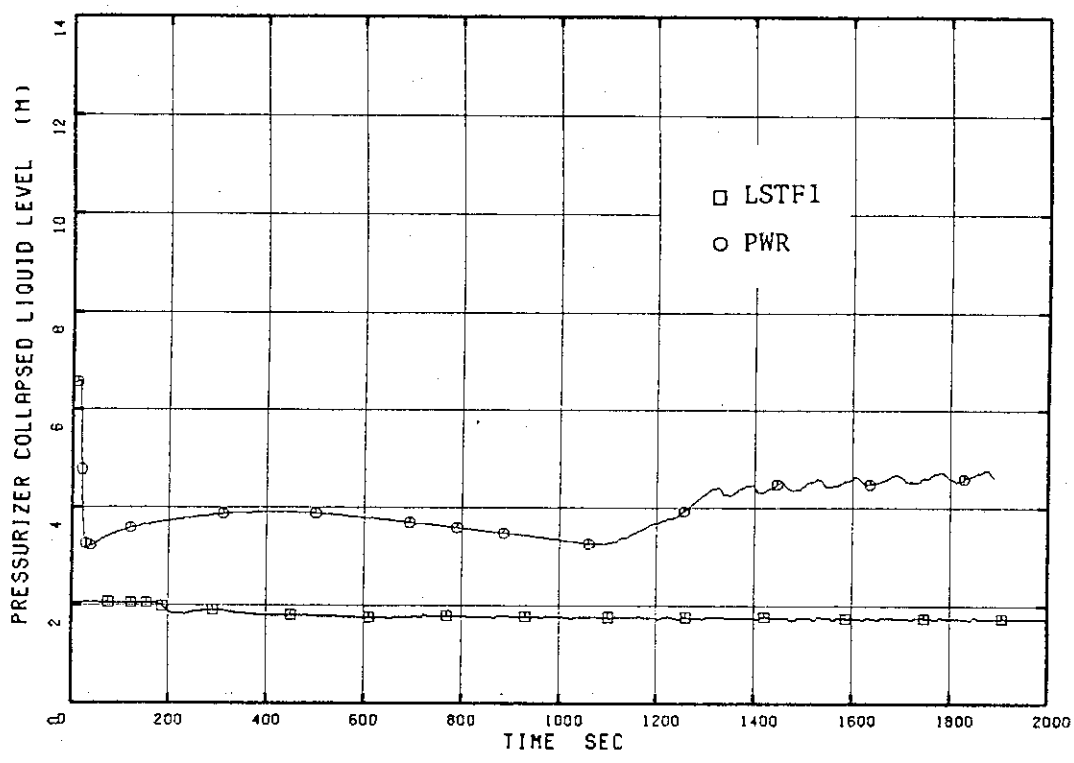

Fig. 4.15 Pressurizer Collapsed Liquid Level - LOFW-C

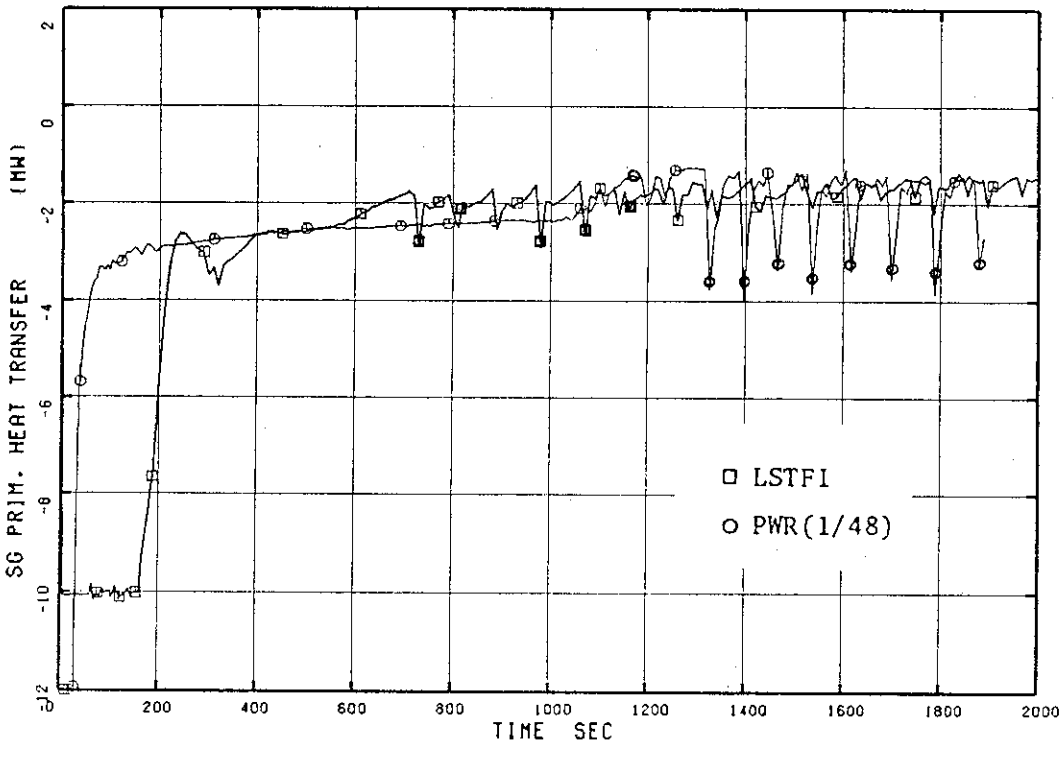

Fig. 4.16 Primary System Heat Removal in the Steam Generators - LOFW-C

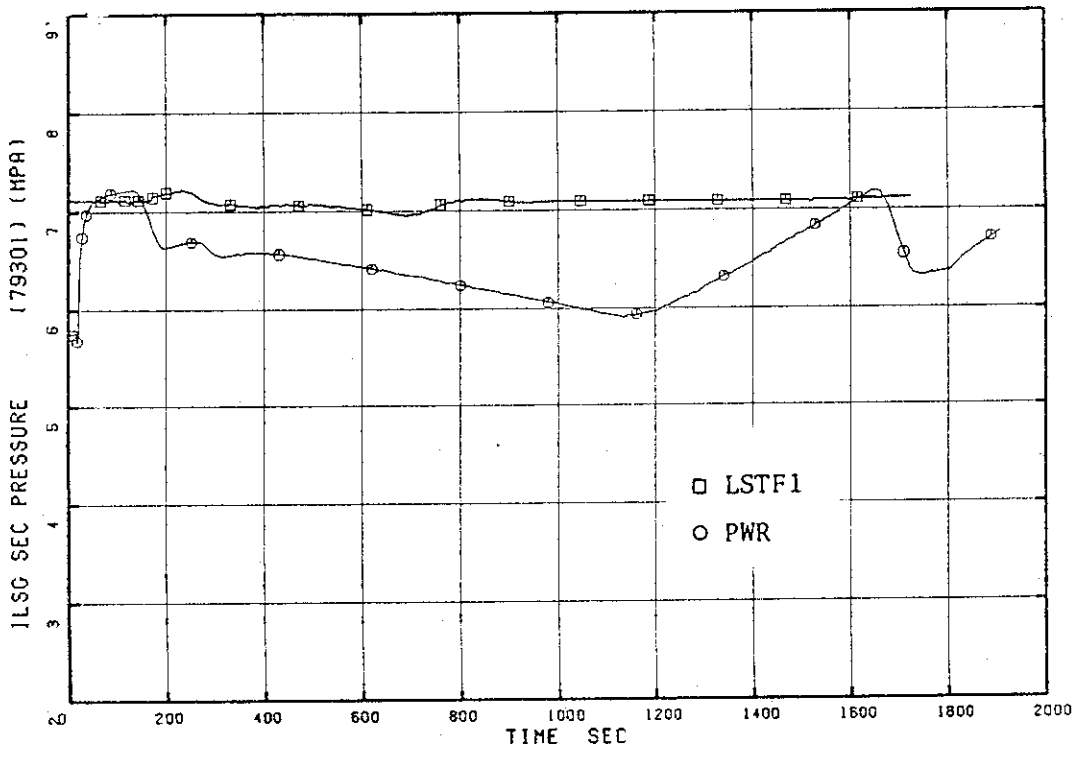

Fig. 4.17 Intact Loop Steam Generator Secondary Pressure - LOFW-D

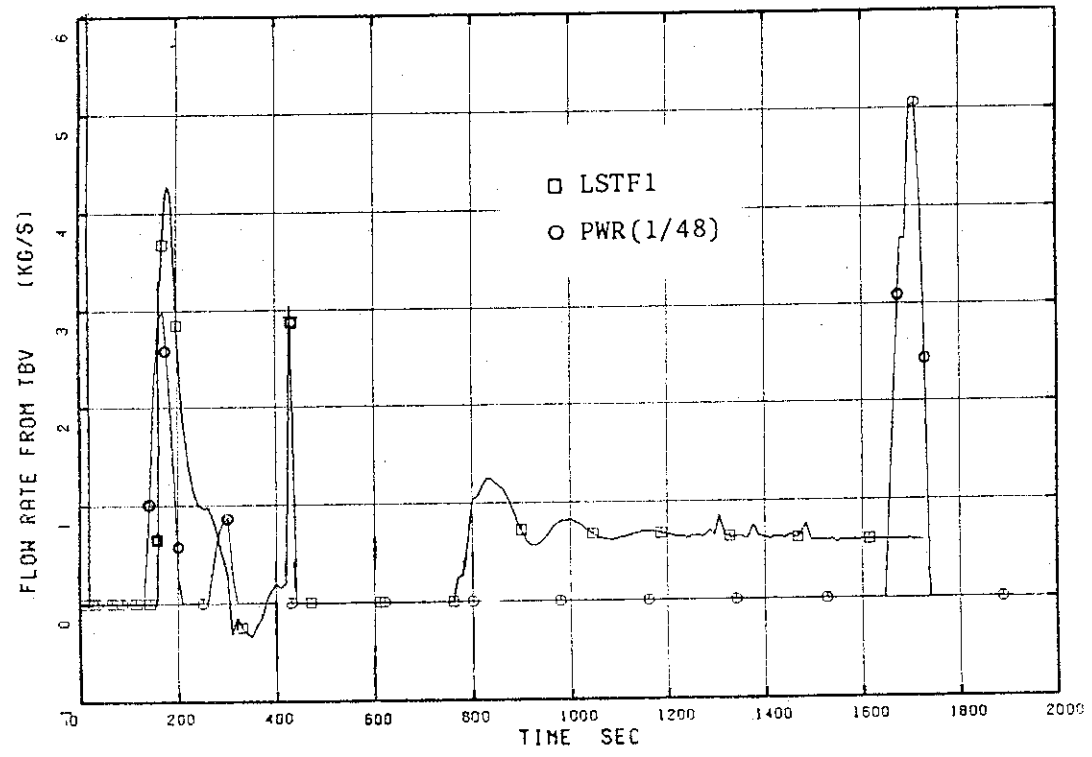

Fig. 4.18 Turbine Bypass Valve Flow Rate - LOFW-D

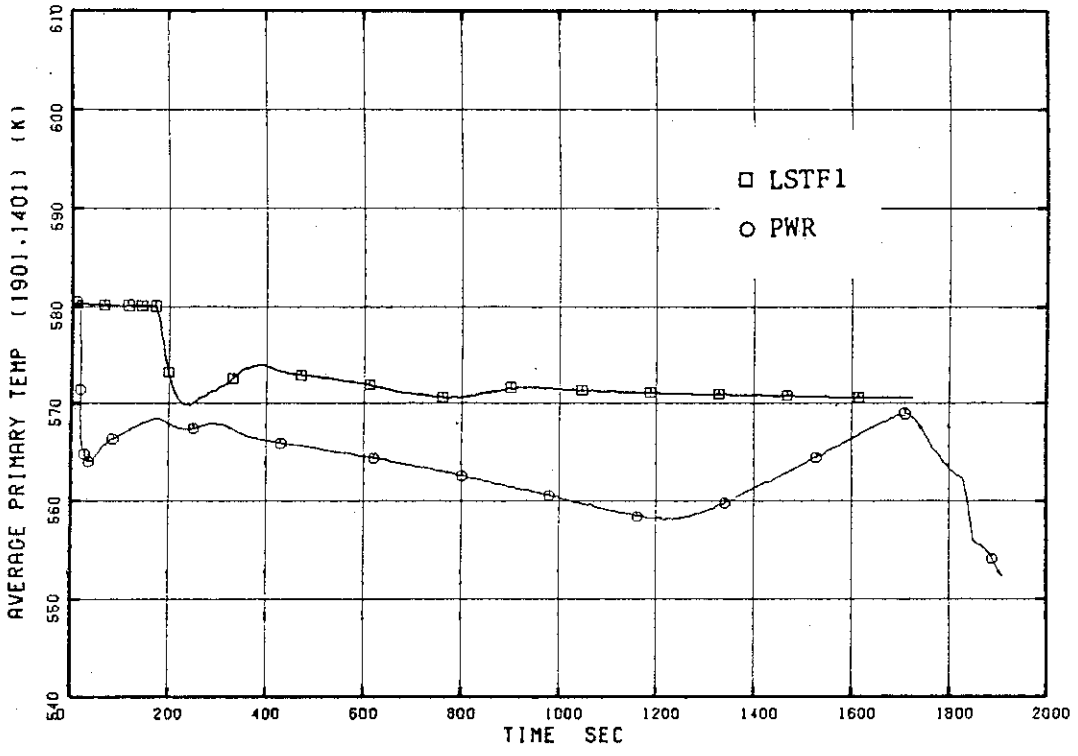

Fig. 4.19 Primary Mean Temperature - LOFW-D

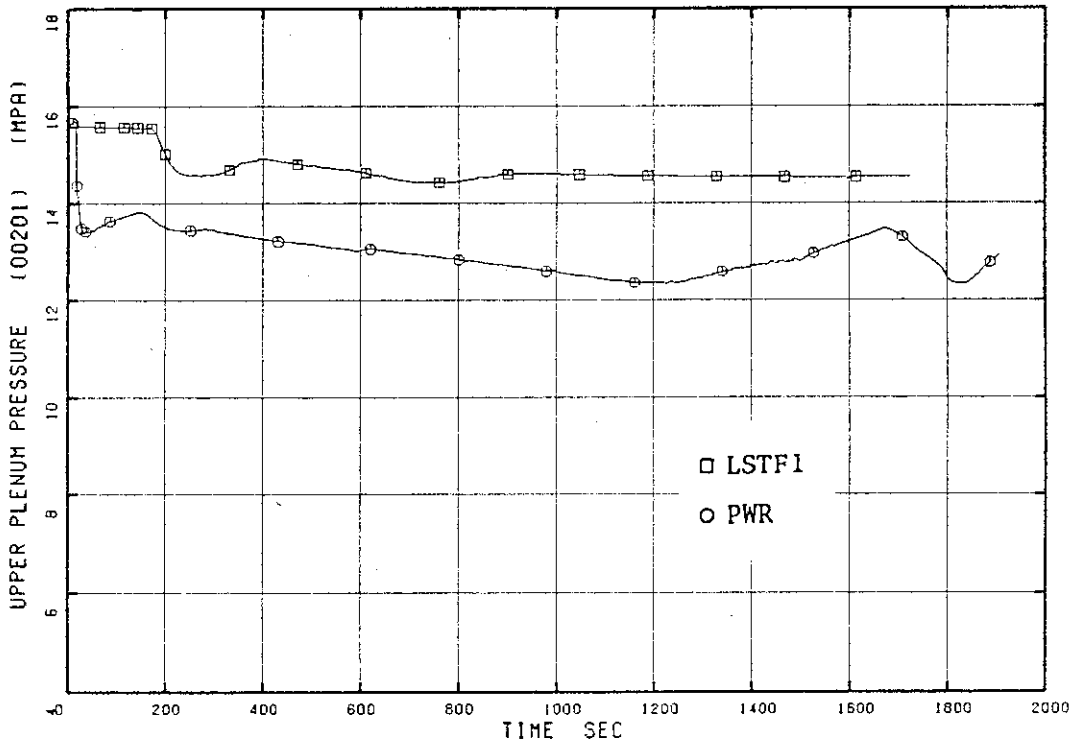

Fig. 4.20 Upper Plenum Pressure - LOFW-D

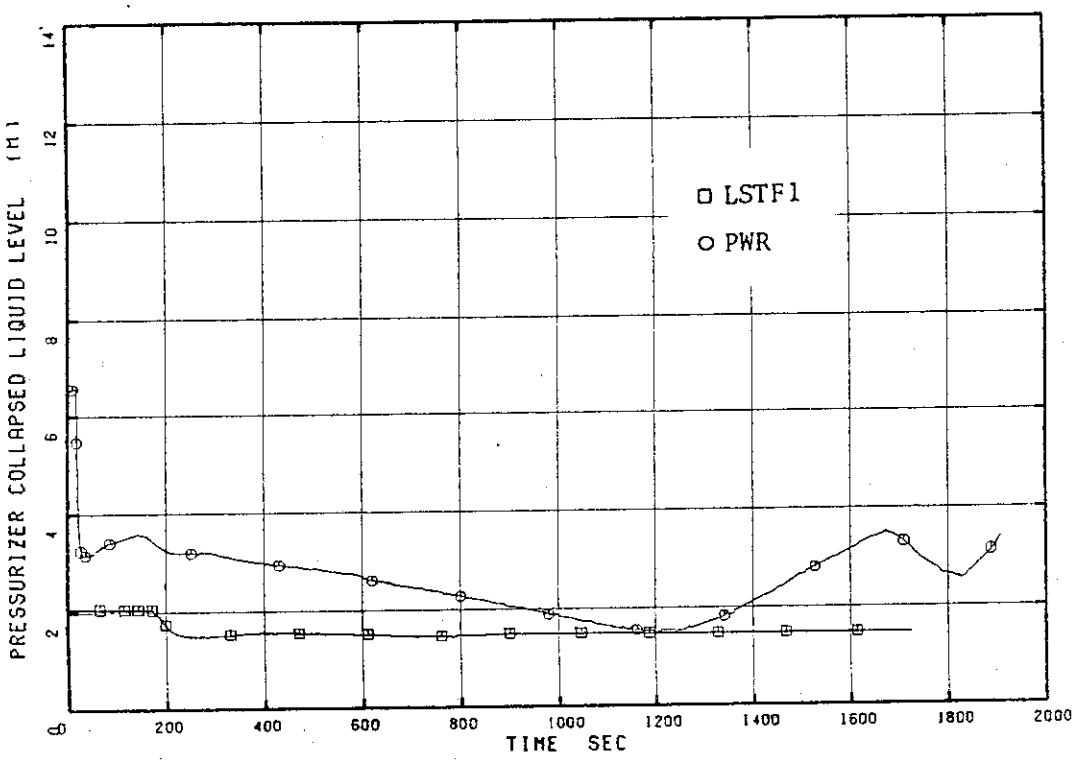

Fig. 4.21 Pressurizer Collapsed Liquid Level - LOFW-D

5. CONCLUSIONS

In this section the main conclusions drawn from the study are presented. In Sections 5.1 to 5.4 the conclusions for each LOFW transient are presented and in Section 5.5 some general conclusions and recommendations are given.

5.1 Conclusions for LOFW-A

The calculations for LOFW-A with LSTF1, LSTF2 and the PWR model showed that LSTF has the capability to simulate the basic response of the PWR to the base case transient. All the runs indicated the primary system would reach hot standby and would be cooled by a secondary feed and bleed through the aux. FW and turbine bypass valve. Differences in core power, SG secondary mass and primary flow rate, however, affected the timing of events in the calculations as well as the details of the system response such as the calculated pressure and temperature.

The main effect of using a smaller secondary mass in LSTF2 compared to LSTF1 was to shift the timing of events closer to the PWR calculation, although they were still not in agreement because of core power differences. The calculations with LSTF2, the model with the initial low SG downcomer level, indicated some thought must be given to determining the scram setpoint if this approach is to be actually used in LSTF.

5.2 Conclusions for LOFW-B

One of the most important items to be calculated in LOFW-B was the time to steam generator dryout. In the three calculations completed for this transient, the time to SG dryout was different due to differences in the amount of mass left in the steam generators at scram. The calculated order of SG dryout was the PWR model, LSTF2 and LSTF1. Differences in the amount of mass remaining in the steam generators at scram for LSTF1 compared to LSTF2 and the PWR model were due to differences in initial mass inventory and in core power for LSTF2 compared to the PWR model. The use of the scaled secondary mass in LSTF2 resulted in an earlier dryout time when compared to LSTF1 but it was still later than in the PWR run because of core power differences. Another factor which affected the time of SG dryout was the greater pump energy input to the

primary fluid in the PWR calculation relative to the LSTF runs because of the smaller pumps in LSTF.

With the earlier steam generator dryout time in the PWR calculation, the primary fluid heated to a higher temperature than in the LSTF runs. At the end of the PWR calculation the subcooling in the hot leg was about 11 K versus 16 K and 23 K in the LSTF runs. This indicates the importance of calculating the dryout time accurately since the amount of subcooling indicates how much more energy can be input to the fluid before voiding begins. In addition, the LSTF runs had a slightly higher heatup rate than the PWR analysis because heat structures were used to represent the pressure vessel wall in the PWR run but not the LSTF runs. These heat structures acted as an additional heat sink in the PWR analysis and, therefore, the fluid heated up at a slower rate. The effect of these additional heat structures indicates the importance of modeling the system metal mass accurately in order to represent the system heat sources and sinks. It also indicates the possible influence of system heat losses on the calculated results for both LSTF and the PWR since these have not been included in either model.

In order to simulate the pressure decrease in the steam generators at dryout, the jet condenser pressure in the LSTF runs was reduced at PWR scram to 3.0 MPa. This introduced oscillations into the calculations not seen in the PWR run or the LSTF base case calculations. The time of scram was chosen to reduce the jet condenser pressure because this was a known trip point. Scram occurred early in the calculations, however, compared to the time of dryout. It is recommended, therefore, that alternative trip points for reducing the jet condenser pressure be investigated which would occur later in the transient and thus delay the introduction of oscillations into the LSTF analyses. Other possibilities for eliminating the oscillations include: (1) adding some resistance to the TBV line to compensate for the larger pressure difference across the TBV with the reduced jet condenser pressure, (2) not reducing the jet condenser pressure and developing alternative methods for monitoring SG secondary mass inventory to determine the time of dryout and therefore the time for MSIV closure, HPI initiation and PCP trip or (3) adjusting the control system in LSTF to compensate for the slower response of the primary mean temperature.

As in the analyses of LOFW-A, differences in core power and primary flow rate affected the time of scram and the details of the system response between the calculations for LSTF and the PWR.

5.3 Conclusions for LOFW-C

Overall, the assumption of turbine bypass valve failure had a greater affect on the LSTF1 calculation than on the PWR run because of the higher initial secondary pressure. With the turbine bypass valve assumed to fail in LOFW-C, energy removal was through the secondary relief valves in both the PWR and LSTF1 analyses. With the initial, higher secondary pressure in LSTF1, the relief valve cycled once shortly after scram whereas, in the PWR analysis, the secondary pressure turned over after scram without challenging the relief valve early in the transient. The higher, initial secondary pressure and the assumption of TBV failure also resulted in a smaller overall change in the primary pressure in LSTF1 during LOFW-C when compared to the PWR run and the LSTF1 calculations for LOFW-A or LOFW-B. The main affect of the TBV failure on the PWR run was to cause small oscillations in the primary system, as the relief valve cycled, which resulted in the primary pressure decreasing slowly due to condensation in the pressurizer.

Differences in core power and flow rate between LSTF1 and the PWR model also affected the time of scram and the primary mean temperature calculated by the models. Differences in the initial SG mass affected the timing of the calculated sequence of events.

5.4 Conclusions for LOFW-D

In the analysis of LOFW-D, the assumption of primary pump trip at scram affected the PWR results more than those calculated with LSTF1. This was probably because of the greater difference between the pumped and natural circulation flow rates in the PWR calculation than in the LSTF1 run. In the PWR calculation, the natural circulation flow rate was approximately 5% of the pumped flow rate compared to 30% in the LSTF1 run.

The response of LSTF1 to LOFW-D was basically the same as in LOFW-A. The PWR response was different, however, with the smaller primary flow rate affecting the primary mean temperature and the response time of the TBV control system and thus the turbine bypass valve operation. This, in turn, influenced the primary pressure response.

Because of the above difference, the pressure in the PWR run was calculated to drop below the ECCS setpoint and HPI injection initiated.

This was not calculated to occur in the LSTF1 analysis of LOFW-D.

The LSTF1 calculation for LOFW-D also indicated careful consideration must be given to the method of jet condenser operation, e.g., when to reduce the jet condenser pressure. The jet condenser pressure was not reduced for the calculation of this transient. However, analysis of the results indicated the steam line check valves closed for several hundred seconds during the transient, because the SG pressure dropped below the jet condenser pressure. This prevented the TBV from removing energy from the system even though it was open. Also, a reduced jet condenser pressure would also have been a more accurate representation of the PWR boundary condition in this transient and the LSTF1 model would probably have calculated more accurately the secondary pressure transient of the PWR run (based on the oscillations calculated with the LSTF1 model in the LOFW-B analysis when the jet condenser pressure was reduced).

5.5 General Conclusions and Recommendations

Based on the results of the loss-of-feedwater transients analyzed in this report, LSTF has the capability to simulate the basic PWR response to a simple loss-of-feedwater as in LOFW-A, the base case analysis. Therefore, the LSTF data are useful for the assessment of the code. When a second system was assumed to fail, however, the analyses showed that the LSTF response and the PWR response could be considerably different.

One factor that affected the response of LSTF in several of the transients was the difference in primary flow rates between the systems. It is recommended, therefore, that if funds become available in the future, serious consideration be given to upgrading the LSTF pumps to be capable of maintaining the full-scaled PWR flow rate.

As would be expected, the calculations of LOFW-B showed the time to steam generator dryout was an important event to represent accurately both analytically and experimentally. Although an attempt was made in this study to calculate the time of this event more accurately by using a scaled secondary mass in the LSTF2 run, there was still some delay in the time of SG dryout over the PWR run. Further analysis of this problem is recommended.

Because of the effect of the additional heat structures modeled in the PWR run on the fluid heatup rate after SG dryout in LOFW-B, it is recommended that more detailed modeling of the system metal mass in LSTF

and the PWR be made. In addition, it is recommended that an evaluation of system heat losses in both LSTF and the PWR be made and model changes made to include these heat losses where appropriate.

The analyses also showed that it is not always clear, a priori, in which transients the LSTF response would better represent the PWR response if the jet condenser pressure were reduced. LOFW-B was one transient where it quickly became clear a reduced jet condenser pressure was needed in LSTF. In LOFW-D, only a careful analysis of the LSTF1 calculated results with the jet condenser pressure held constant indicated the calculated response might have been improved by reducing the jet condenser pressure. It is recommended that a calculation using LSTF1 with a reduced jet condenser pressure be made in the future to check and see if this is true.

Careful consideration must be given in determining trip points in LSTF if there is not a corresponding PWR trip or if other factors influence this decision. This was illustrated in the analyses by the problems encountered in determining the scram setpoint in the LSTF2 model, when the scaled secondary mass was used, and by the oscillations which were calculated in the LSTF runs for LOFW-B when the jet condenser pressure was reduced. Investigation of alternatives to the choices made in completing these calculations could result in an improved calculation for LSTF when compared to the PWR.

In general, the calculations in this report represent a first attempt to compare the calculated response for LSTF and the PWR to a LOFW. A few of the problems encountered in making the calculations have been addressed although none have been completely answered. This report, therefore, should not be viewed as a final statement of the capability of LSTF to simulate the PWR response to a LOFW, but rather as a point of reference from which to begin further study and analysis. As this study and analysis gives better choices for trip setpoints, control systems and methods of operation, the calculated response of LSTF, relative to the PWR, should improve.

ACKNOWLEDGEMENTS

The Authors are grateful to Dr. Y. Koizumi and Dr. Y. Kukita for their helpful discussions on the LOFW analyses and their review of the text of this report.

REFERENCES

1) Nakamura, H., et al., "System Description for ROSA-IV Two-Phase Flow Test Facility (TPTF)," JAERI-M 83-042 (1983).
2) Tasaka, K., et al., "Conceptual Design of Large Scale Test Facility (LSTF) of ROSA-IV Program for PWR Small Break LOCA Integral Experiment," JAERI-M 9849 (1981).
3) Tanaka, M., Katada, K. and Tasaka, K., "Preanalysis of ROSA-IV LSTF for PWR Small-Break LOCA Test with RELAP5/MOD0 - 10% Cold Leg Break with HPI Failure," JAERI-M 9356 (1981).
4) Tanaka, M., Katada, K., and Tasaka, K., "Preanalysis of ROSA-IV LSTF for PWR Small-Break LOCA Test with RELAP5/MOD0 - 2.5% Cold Leg Break with HPI Failure," JAERI-M 9676 (1981).
5) Tanaka, M., Fineman, C. and Tasaka, K., "PORV Break Calculations for the ROSA-IV LSTF and the Reference PWR with RELAP5/MOD1 (cycle 1)," TO BE PUBLISHED.
6) Ransom, V.H., et al., "RELAP5/MOD1 Code Manual, Volumes 1 and 2," EGG-2070 (1982).

ACKNOWLEDGEMENTS

The Authors are grateful to Dr. Y. Koizumi and Dr. Y. Kukita for their helpful discussions on the LOFW analyses and their review of the text of this report.

REFERENCES

1) Nakamura, H., et al., "System Description for ROSA-IV Two-Phase Flow Test Facility (TPTF)," JAERI-M 83-042 (1983).
2) Tasaka, K., et al., "Conceptual Design of Large Scale Test Facility (LSTF) of ROSA-IV Program for PWR Small Break LOCA Integral Experiment," JAERI-M 9849 (1981).
3) Tanaka, M., Katada, K. and Tasaka, K., "Preanalysis of ROSA-IV LSTF for PWR Small-Break LOCA Test with RELAP5/MOD0 - 10% Cold Leg Break with HPI Failure," JAERI-M 9356 (1981).
4) Tanaka, M., Katada, K., and Tasaka, K., "Preanalysis of ROSA-IV LSTF for PWR Small-Break LOCA Test with RELAP5/MOD0 - 2.5% Cold Leg Break with HPI Failure," JAERI-M 9676 (1981).
5) Tanaka, M., Fineman, C. and Tasaka, K., "PORV Break Calculations for the ROSA-IV LSTF and the Reference PWR with RELAP5/MOD1 (cycle 1)," TO BE PUBLISHED.
6) Ransom, V.H., et al., "RELAP5/MOD1 Code Manual, Volumes 1 and 2," EGG-2070 (1982).

Appendix: LSTF HPI Pump FLow Rate Sensitivity Study

The high pressure injection (HPI) pumps in LSTF will have a maximum flow rate capability greater than the full-scaled flow rate of the HPI pumps in the PWR. To study the effect of using the LSTF pumps at full capacity on LOFW-B, a calculation was run with LSTF1 where the pressure vs. flow tables of the time dependent junctions representing the HPI pumps were changed to reflect the full capacity of the LSTF pumps. This model was designated LSTF1-A.

The system response calculated by LSTF1-A was the same as LSTF1 out to the time of steam generator dryout. The only difference after this time was that, with the higher HPI flow rate in LSTF1-A, sufficient ECCS was injected into the system to cool the primary fluid. This is shown in Figure A.1 which compares the PWR, LSTF1 and LSTF1-A primary mean temperatures. The mean temperature in the PWR and LSTF1 increased after SG dryout because the ECCS flow at the PORV septoint was not sufficient to cool the fluid. The primary mean temperature in LSTF1-A, however, decreased.

Based on these results, some means of controlling the pressure vs. flow curve of the LSTF HPI pumps is needed in order to simulate the PWR response.

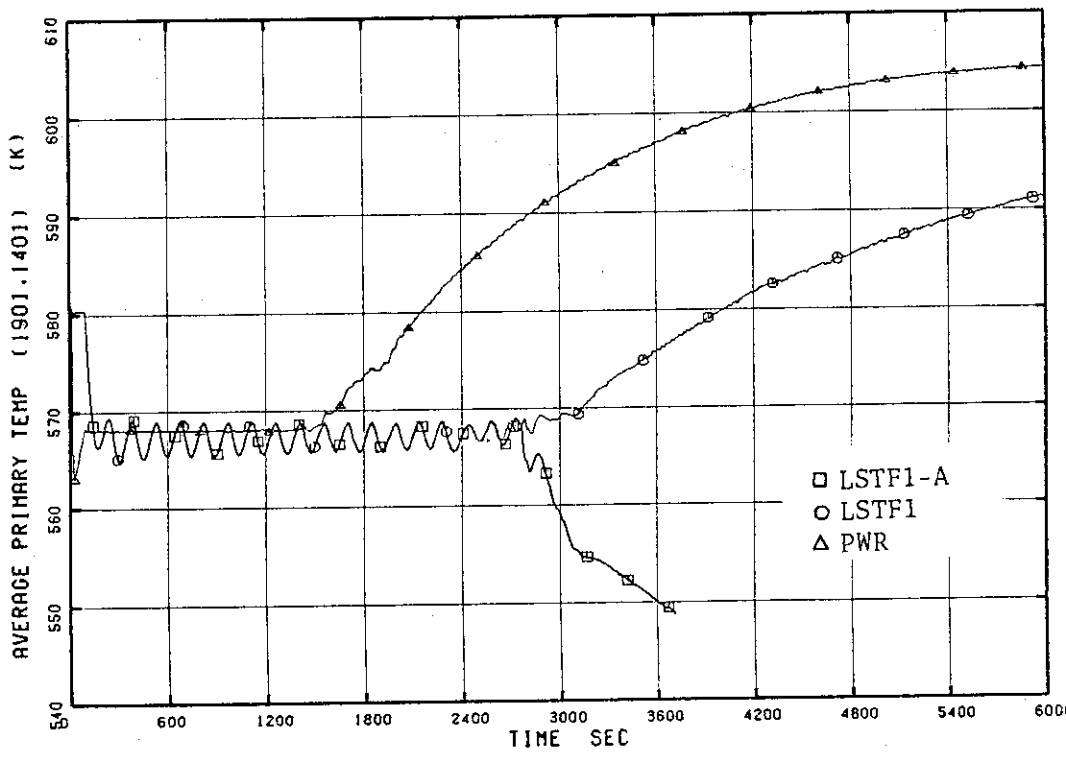

Fig. A.1 Primary Mean Temperature for LOFW-B: PWR, LSTF1 and LSTF1-A